

# We are IntechOpen, the world's leading publisher of Open Access books Built by scientists, for scientists

6,900

Open access books available

186,000

International authors and editors

200M

Downloads

Our authors are among the

154

Countries delivered to

TOP 1%

most cited scientists

12.2%

Contributors from top 500 universities



WEB OF SCIENCE™

Selection of our books indexed in the Book Citation Index  
in Web of Science™ Core Collection (BKCI)

Interested in publishing with us?  
Contact [book.department@intechopen.com](mailto:book.department@intechopen.com)

Numbers displayed above are based on latest data collected.  
For more information visit [www.intechopen.com](http://www.intechopen.com)



# Nd-Fe-B Nanocomposite Thin Films: Influence of the Additions on the Structure and Hard Magnetic Properties

Urse Maria, Grigoras Marian, Lupu Nicoleta and Chiriac Horia  
*National Institute of Research and Development for Technical Physics, 700050 Iasi,  
Romania*

## 1. Introduction

Nd-Fe-B thin films have been extensively investigated as promising candidates for Micro-Electro-Mechanical Systems (MEMS) and in monolithic microwave integrated circuits (Walther et al., 2009, 1991; Lemke et al., 1995).

The Nd-Fe-B nanocomposite hard magnetic materials consist of suitably nanodispersed hard (i.e. Nd<sub>2</sub>Fe<sub>14</sub>B) and soft (i.e.  $\alpha$ -Fe or Fe<sub>3</sub>B) phases that are exchange coupled (Ao et al., 2006) and confer them specific magnetic properties with potential great impact on the permanent magnet market, such as enhanced technical performances (Wang et al., 2007) and low cost. Thus, in nanocomposite magnets, the best properties of the soft and hard magnetic phases are combined via exchange coupling on a nanometric scale (Ghidini et al., 2007).

The crystallographic structure of the nanocomposite hard magnetic magnets plays a more important role in controlling the magnetic properties than in single-phase magnets (Cui et al., 2000). Thus, the refinement of the microstructure and uniform distribution of the component phases are essential to obtain high coercivity,  $H_c$ , and high maximum energy products  $(BH)_{max}$ . (Chen et al., 2006). The optimization of microstructure and magnetic properties of Nd-Fe-B films can be obtained by compositional and phase modifications with additions of dopant elements (Jiang and O'Shea, 2000). Many metallic elements have been added to the ternary Nd-Fe-B system with the aim of improving the microstructure and magnetic properties (Cui et al., 2000; Chang et al., 2008, 2009). The Nd-Fe-B thin films deposited on substrates maintained during deposition at room temperature, in as-deposited state and after thermal treatments at temperatures below 550°C, have amorphous structure. During the annealing at higher temperatures, high melting point metal dopants (i.e. Nb, Zr, Mo, Ti, V, etc) act as nuclei for crystallization process, thus impeding grain growth upon initial annealing. Low melting point metal dopants (i.e. Cu, Al, Ga, In, Zn, etc) surround the magnetic phase grains in the course of crystallization, hindering their growth. Thus, in Nd-Fe-B alloys with the best magnetic properties, either or both types of such elements are usually added (Shandong et al., 2002; Chang et al., 2009). In order to enhance the intrinsic properties of the magnetic phases, other elements, such as rare-earth elements (i.e. Dy, Pr, La, Tb, Sm), are partially substituted for Nd (Shandong et al., 2002; Liu et al., 2003), transition elements, (i.e. Co, Mn), are partially substituted for Fe (Cui and O'Shea, 2003; Cui and O'Shea, 2004), and C partially replaces B (Ishii et. al., 2007).

Nanocomposite magnets exhibit a high remanence,  $M_r$ , and a large coercive field,  $H_c$ , if hard and soft phases are adequately exchange coupled. Remanence enhancement was observed in multilayered ( $\alpha$ -Fe, Fe<sub>3</sub>B)/Nd-Fe-B magnets because of the exchange coupling between soft and hard magnetic phases (Liu et al., 2003). Various multilayered systems, such as  $\alpha$ -Fe/Nd<sub>2</sub>Fe<sub>14</sub>B (Cui et al., 2000; Wang et al., 2007), Fe<sub>3</sub>B/Nd<sub>2</sub>Fe<sub>14</sub>B (Rajasekhara et al., 2008) or Fe-Co/Nd<sub>2</sub>Fe<sub>14</sub>B (Ao et al., 2006), with different thickness of constituent layers and grain size ratio of soft and hard magnetic phases were tested to determine the most optimum morphology of thin-film nanocomposite magnets with enhanced remanence.

As compared to isotropic single-phase nanocrystalline Nd-Fe-B magnets, the coercive field obtained in two-phase systems is rather low. Recent studies demonstrated that the addition of different transition metal elements with high and low melting points to the ternary Nd-Fe-B alloy is an effective method also for the hard magnetic properties improvement (Cui et al., 2000; Tsai et al., 2002; Ping et al., 2000; Shull, 2007).

The additives or substitutions were either included either within the Nd-Fe-B films volume or by stratification as spacer layers. The microstructure and magnetic properties of the multilayered systems can be well controlled by varying the thickness of the soft and hard magnetic layers. Studies have been also reported on the influence of singular and multiple additions such as, Co, (Nb and Cu), and (Fe and Si), the thickness of component layers and annealing conditions on the structure and hard magnetic properties of multilayered [Nd-Fe-B/(Nb-Cu)] $\times$ n (a-Chiriac et al., 2007), [Nd-Fe-B-Nb-Cu/Co] $\times$ n (b-Chiriac et al., 2007) and [Nd-Fe-B-Nb-Cu/Fe-B-Si] $\times$ n (Chiriac et al., 2008) thin films. The Nb and Cu additions act in the sense of impeding the grain growth and promoting the formation of nucleation sites, respectively (Chiriac et al., 1999; Tsai et al., 2002, 2000; Wang et al., 2005; Ping et al., 2000 and 1999), Co increases the Curie temperature and boosts the crystallization and grain growth (Cui and O'Shea, 2003, 2004; Jurczyk and Jakubowicz, 2000; Chiriac and Marinescu, 1998), whereas Si slightly increases the Curie temperature and improves the rectangularity of the demagnetization curves (Coey, 1996; Xiong et al., 2002).

In this chapter the results with regard to the magnetic properties of Nd-Fe-B nanocomposite permanent magnet thin films (single layer and multilayer) with addition of Cu, Nb and Si, respectively, and Co substitution for Fe, are presented. The results concerning the effect of the thickness of constituent layers and annealing conditions on the structure, hard magnetic properties and exchange coupling between hard and soft magnetic phases composing the nanocomposite Nd-Fe-B thin films are comparatively discussed. The thermal stability evolution as a result of thermal cycling in the temperature range 25-350°C for Nd-Fe-B, Nd-Fe-B-Nb-Cu and [Nd-Fe-B-Nb-Cu/Co] $\times$ 3 thin films is also presented. The influence of the ageing for different periods of time at 150°C, on the losses in coercivity,  $H_c$ , and remanent magnetization,  $M_r$ , has been also studied and will be discussed in detail (Chiriac et al., 2009).

## 2. Nd-Fe-B nanocomposite thin films processing

Generally, the Nd-Fe-B thin films are prepared by different vacuum deposition techniques, such as magnetron r.f./d.c sputtering, ion-plasma sputtering, molecular beam epitaxy, laser ablation, etc.

Our buffer/Nd-Fe-B/capping thin-film samples without or with additions (single layer and multilayer) were prepared, in vacuum, by sequential deposition in a conventional deposition system (Laboratory Sputtering Plant Z – 400) using r.f sputtering and electron beam evaporation techniques. The simple or composite sputtering targets were mounted on

two separate guns and were made as follows: a disc of stoichiometric Nd-Fe-B alloy with Nd and other addition chips on its surface; a disc of specific materials for 'buffer' or 'capping' layers (i.e. Ta, Nb or Nb-Cu); a disc of Nb-Cu combination or Fe-Si-B alloy, for spacer layer.

Usually, during Nd-Fe-B thin film deposition, a Nd supplementary amount is required to be added to compensate oxidation of Nd. Generally, compositional changes of samples were made by modifying the surface of the components on the sputtering targets, or by modifying the thicknesses of hard and soft layers of multilayer systems.

The soft magnetic (i.e. Co) thin films were prepared in vacuum using electron beam evaporation technique.

The substrate temperature during the deposition of thin films is the first important parameter of this technological process. The Nd-Fe-B films are amorphous when the substrate temperature is lower than the main phase Nd<sub>2</sub>Fe<sub>14</sub>B crystallization temperature (Lileev et al., 2002).

The sputtered samples were deposited, at room temperature, in high purity (99.999%) argon (Ar) atmosphere at working pressure of about 10<sup>-2</sup> mbar. The background pressure of the vacuum chamber was about 2x10<sup>-6</sup> mbar. The distance between sputtering target and substrates was of about 3.2 cm.

The thickness of the individual layers prepared by electron beam evaporation techniques (i.e. Co), was controlled during the deposition process by a quartz-crystal deposition monitor (FTM 6 Film Thickness Monitor) having a resolution of about 0.1 nm. When r.f sputtering was used as deposition technique, the thickness of the individual films was verified 'ex-situ' by the KLA Tencor Alpha - Step IQ Profilometer. Thus, the thickness of each sputtered layer from multilayer system was monitored during the deposition process by controlling the sputtering time.

The magnetic and thermo-magnetic measurements were performed at room temperature and in the temperatures range 25 ÷ 900°C, respectively, by a vibrating sample magnetometer (Lake Shore VSM 7410) with a maximum magnetic field of 31 kOe applied parallel with the film plane.

The crystallographic structure was investigated using X-ray diffraction (XRD) analysis. A X-ray diffractometer (Bruker AxS GmbH - D8 Advance) with a monochromatized Cu-K $\alpha$  radiation was used in a Bragg-Brentano arrangement. The Warren-Averbach method (Klug and Alexander, 1974) was used to estimate the crystalline grain sizes (error of  $\pm 15\%$ ).

The film composition of the individual films was obtained by using the SEM/EDS (Scanning Electron Microscopy - JEOL JSM 6390, and associated Energy - Dispersive Spectrometry) technique.

The morphology of the samples was investigated by Transmission Electron Microscopy (TEM) technique using molybdenum 'microscope grids' coated with an evaporated carbon thin film having the thickness between 8 and 10 nm.

The Nd<sub>2</sub>Fe<sub>14</sub>B/( $\alpha$ -Fe, Fe<sub>3</sub>B) nanocomposite structure is usually obtained by controlled crystallization of amorphous phase. DSC studies shown that nucleation temperatures of the  $\alpha$ -Fe and Nd<sub>2</sub>Fe<sub>14</sub>B phases are of about 525°C and 590°C, respectively (Cui et al., 2005). In order to crystallize the Nd<sub>2</sub>Fe<sub>14</sub>B and soft magnetic phases and obtain good hard magnetic properties, the Nd-Fe-B thin-film samples can be subjected after deposition, to two types of annealing procedures. Thus, the as - deposited samples can be treated in vacuum ( $p = 4 \times 10^{-4}$  Pa) by rapid (30 second) or standard (10-30 minutes) annealing at temperatures between 550°C and 780°C. A rapid annealing of about 30 s at a higher temperature allows more nucleation centers to form and grow during the crystallization process of the as-

deposited films. Comparing with a longer time and lower temperature annealing, it is expected that a rapid annealing would lead to more uniform grain size for both the hard and soft phases and sharper interface boundaries (Cui and O'Shea, 2004).

Other types of thermal treatment procedures have been also proved to be effective in improving the magnetic performance of nanocomposite permanent magnet materials. Cui and co-workers (2005) studied the influence of magnetic field annealing on the magnetic properties of  $\text{Nd}_{2.4}\text{Pr}_{5.6}\text{Dy}_1\text{Fe}_{84}\text{Mo}_1\text{B}_6$  ribbons. Compared with the sample annealed without a field, there is a noticeable improvement in the magnetic properties for the magnetically annealed samples, especially of the energy product  $(BH)_{max}$ . This improvement is a result of the enhanced crystallographic texture, nanostructure refinement, and in-plane uniaxial magnetic anisotropy. Similar effect may be expected in thin films.

In the course of our own research studies, different compositions of Nd-Fe-B target were tested in view of obtaining the Nd-Fe-B thin films with optimum hard magnetic properties. The composition of the Nd-Fe-B thin films was adjusted by changing the numbers of Nd chips on the surface of the sputtering target. The optimum hard magnetic properties of Nd-Fe-B thin films were obtained when the following composition of sputtering target was used: disc of  $\text{Nd}_{12}\text{Fe}_{82}\text{B}_6$  alloy with the diameter of 7.5 cm having on its surface Nd chips with the a total area of about 4.9  $\text{cm}^2$  and B chips with the a total area of about 5.3  $\text{cm}^2$ . The composition of Nd-Fe-B(540nm) film obtained by SEM/EDS technique is as follows: Fe 77.23 at.%, Nd 15.02 at.%, B up to 100 at.%.

The structure and magnetic properties of thin films can be strongly influenced by the interaction between the film and the substrate or (if present) buffer layer. Capping layer has also an important influence on the hard magnetic characteristics of Nd-Fe-B thin films. Several materials (such as Cr, Mo, Nb, Ta, Ti, V, etc.) were used between the Nd-Fe-B layer and the substrate to protect the Nd-Fe-B from oxidation by any oxygen in oxide form located on the substrate, and to control the growth of the  $\text{Nd}_2\text{Fe}_{14}\text{B}$  phase. Usually, same materials are used as protective over layers since they are mechanically hard and form stable oxides, and moreover, the rare earths (i.e. Nd) have a low solubility in the respective oxide compounds (Jiang and O'Shea, 2000).

In our experiments, all the samples were sandwiched between two Ta layers with the thickness of 40 nm and 20 nm, which were used as buffer layer and capping layer, respectively. Occasionally, we used two Nb-Cu films with the thickness of about 20 nm as buffer layer and capping layer.

### 3. Relationship between the magnetism of $\text{Nd}_2\text{Fe}_{14}\text{B}/(\alpha\text{-Fe, Fe}_3\text{B})$ and microstructure

In nanocomposite permanent magnets the structure plays an important role on the magnetic properties than in single phase magnets. Generally, the optimum nanostructure of thin-film nanocomposite magnets consists of uniformly distributed hard magnetic and soft magnetic or non-magnetic phase grains.

The permanent magnet properties of nanocomposite alloys based on rare earth - transition metals are determined through the magnetic hardening of the soft magnetic grains based on Fe by the  $\text{Nd}_2\text{Fe}_{14}\text{B}$  hard magnetic neighboring grains. The optimum behavior of  $\text{Nd}_2\text{Fe}_{14}\text{B}/(\alpha\text{-Fe, Fe}_3\text{B})$  nanocomposite alloys as hard magnetic materials originates in the magnetic interactions between the uniformly distributed hard ( $\text{Nd}_2\text{Fe}_{14}\text{B}$ ) and soft ( $\alpha\text{-Fe, Fe}_3\text{B}$  and other) magnetic grains.

Homogenous and textured nanostructures are essential for the achievement of high maximum energy product  $(BH)_{max}$  in nanocomposites (Cui et al., 2005; Manaf et al., 1993). At the same time, the grain size of the soft phase reduced at the same order of magnitude as the double domain wall width of the  $Nd_2Fe_{14}B$  phase allows the exchange interaction between both magnetic phases, thus preserving a high coercivity. In order to achieve this criterion, special attention is necessary to be paid to the formation of the nanocrystalline phases including compositional peculiarities and material preparation procedures (Manaf et al., 1993).

Because the magnetization reversal starts at the grain boundaries where a strongly nonuniform magnetic state exists, the intrinsic magnetic properties of this region strongly influence the remanent magnetization and the coercive field of two phase nanocomposite magnets. The remanent amorphous intergranular phase is expected to reduce the exchange interactions between the hard and soft grains, leading to an improved coercive field (Schrefl et al., 2000).

Fukunga and co-workers (1999) also proposed a two-phase microstructure consisting of Nd-Fe-B and  $\alpha$ -Fe or  $Fe_3B$  grains embedded within a residual amorphous phase. With the same reason as described above, increase of the coercive field without a significant loss of the remanent magnetization enhances the energy density product (Schrefl et al., 2000).

Thin-film NdFeB/ $\alpha$ -Fe nanocomposite magnets consisting of dispersed hard and soft magnetic phases with the grain size in the 10-30 nm range have been reported (Shindo et al., 1997; Yang and Kim, 1999) with high reduced remanent magnetization and magnetic energy product. These materials have wide application as permanent magnets and are useful in micro-mechanical devices (Walther et al., 2009) and may have numerous applications in magneto-electronic devices.

Generally, all the as-deposited and below 550°C annealed Nd-Fe-B thin films have  $H_c$  values of up to 200 Oe. Annealing at 550°C or higher, results in the formation of the hard  $Nd_2Fe_{14}B$  phase responsible for the coercivity increase. XRD investigations demonstrate that the Nd-Fe-B thin films annealed at temperatures of about 550°C are composed of a structural mixture in which a small amount of  $\alpha$ -Fe and  $Nd_2Fe_{14}B$  nanocrystallines are embedded in an amorphous matrix. Annealing at 650°C or higher for 20 minutes leads to the formation of a composite structure consisting of  $\alpha$ -Fe and  $Nd_2Fe_{14}B$  phases.

To obtain a more ideal structure with a uniform distribution of the soft and hard phases, a multilayer system with alternating soft and hard magnetic layers was prepared by using of successive vacuum depositions. In such materials there is a trade-off between the magnetization increase and coercivity decrease as the amount of the soft phase is increased (Cui and O'Shea, 2004). In this nanostructured form there is a large interface contact area between soft and hard grains leading to a strong interface magnetic exchange effect which couples the soft and hard component phases. If the size of the soft phase is comparable with the double domain wall thickness of the hard phase, the two phases reverse together under the influence of a reverse applied field (Cui and O'Shea, 2003).

In contrast to bulk magnets, the structure of the multilayer materials can be easily controlled during the preparation process by properly arranging different layers, adjusting the thickness of the layers of the hard and soft phases, and annealing at the proper temperatures. This leads to an optimized average grain size and grain-size distribution (Ao et al., 2006). In comparison with the single-layer, the remanent magnetization of the multilayer magnets was found to increase noticeably (Liu et al., 2003).

Refinement of the Nd-Fe-B films microstructure to less than 40 nm is essential to obtain the high coercivity and high-energy product  $(BH)_{max}$ . (Miyoshi et al., 2000). A number of specific factors including sample composition, preparation and annealing conditions can affect the microstructure of the thin films and their magnetic properties. A good control of the nanocomposite thin films microstructure can be achieved by architecture (stratification of the hard magnetic layer with magnetic or non-magnetic film used as spacer layer; thicknesses of layers; embedding of hard magnetic grains in a magnetic or non-magnetic matrix) and by additions.

#### 4. Influence of additions on structural and hard magnetic properties

The design of the nanocomposite materials depends on a great number of factors, such as the crystallite size, texture, interfaces volume, etc., which are significantly influenced by the composition, deposition methods and process parameters.

Hirosawa and co-workers (1993) reported that the modification of the alloy composition by microalloying is an effective way of improving the hard magnetic properties of the  $\text{Fe}_3\text{B}/\text{Nd}_2\text{Fe}_{14}\text{B}$  nanocomposite magnets. The main effects of additives and substitutions on the magnetic properties of the nanocomposite magnets originate from modifications of the grain sizes of the soft and the hard magnetic phases (Cui et al., 2000).

Typically, the improvement in the magnetic properties of nanocomposite magnets is a result of the enhanced crystallographic texture, nanostructure refinement, and uniaxial magnetic anisotropy enhancement (Cui et al., 2005).

A commonly way for the preparing of the  $\text{Nd}_2\text{Fe}_{14}\text{B}/(\alpha\text{-Fe}, \text{Fe}_3\text{B})$  nanocomposite magnetic materials is to crystallize an amorphous precursor phase into a mixture of hard and soft magnetic phases (Chang et al., 1999; Cui et al., 2003). In Nd-Fe-B nanocomposite magnets, the replacement of  $\alpha\text{-Fe}$  with  $\text{Fe}_3\text{B}$  improves the coercive field,  $H_c$ , but deteriorates the loop shape (Schrefl and Fidler, 1999). For  $\text{Nd}_2\text{Fe}_{14}\text{B}/\alpha\text{-Fe}$  nanocomposite magnetic materials, the reduction of coercive field is attributed to the emergence of  $\alpha\text{-Fe}$  after annealing. Because, the  $\alpha\text{-Fe}$  and the metastable phases (such as  $\text{Nd}_3\text{Fe}_{62}\text{B}_{14}$ ) usually precipitate from the amorphous precursor earlier than the  $\text{Nd}_2\text{Fe}_{14}\text{B}$  phase, and moreover, the  $\alpha\text{-Fe}$  grains tend to grow coarse during the decomposition of metastable phase therefore leading to weakening of the intergrain exchange coupling, it is important to find a way to change the crystallization behavior of the amorphous phase and to restrain the excessive growth of the soft and hard magnetic grains (Withanawasam et al., 1994).

Nanocomposite permanent magnets require nanostructured grain sizes, especially for the soft magnetic phase. In addition to the grain size of  $\alpha\text{-Fe}$ , the grain size of  $\text{Nd}_2\text{Fe}_{14}\text{B}$  hard magnetic phase is another important factor in determining the magnetic properties of Nd-Fe-B nanocomposite materials (Wang et al., 2007). The optimum average grain size of the  $\alpha\text{-Fe}$  is different for various element substitutions (Cui et al., 2000).

The exchange-coupling interactions between soft and hard grains increase the average anisotropy of soft magnetic grains and decrease the one of hard magnetic grains. In order to get higher effective anisotropy between magnetically soft and hard magnetic grains, the grain size of hard magnetic grain should not be less than 25 nm, and the grain size of soft magnetic grain should be about 10 nm (Sun et al., 2008). The control of grain growth in magnet processing is generally accomplished with non-magnetic additives, at the expense of forming grain boundary phases that reduce interfacial coupling and the overall magnetization

(Hadjipanayis, 1999; Jiang et al., 2004). The optimum average grain size is different for various element substitutions (Cui et al. 2000).

Generally, the additives can be embedded in magnetic thin film volume by two ways: (1) the stratification of magnetic film using additive film as spacer layers and (2) the inclusion of additives direct in the film volume during deposition by co-deposition (i.e. co-sputtering; sputtering out of composite targets). Many metallic elements can be added to the ternary Nd-Fe-B system with the aim of enhancing the magnetic properties. Generally, high melting point metals such as Zr, Nb, Mo, Ti, etc, act as nuclei for crystallization which emerge from the amorphous matrix in the primary stage of crystallization, thus impeding grain growth on initial annealing. These types of additions lead to the refinement of both  $\text{Nd}_2\text{Fe}_{14}\text{B}$  and  $\alpha\text{-Fe}$  phases (Zhang et al., 2009; Chang et al., 2008; Wang et al., 2005 and 2007). Low melting point metals such as copper (Cu) can reduce the crystallization temperature of the alloy (Ping et al., 1999).

#### 4.1 Influence of Nb and Cu additions

Minor addition of copper (Cu) to  $\text{Nd}_{4.5}\text{Fe}_{77}\text{B}_{18.5}$  alloy is effective in refining the  $\text{Fe}_3\text{B}/\text{Nd}_2\text{Fe}_{14}\text{B}$  nanocomposite microstructure that is produced by crystallization of amorphous phase. While single addition of niobium (Nb) shows adverse effect on the grain size of the nanocomposite, combined addition of Cu and Nb to  $\text{Nd}_{4.5}\text{Fe}_{77}\text{B}_{18.5}$  shows beneficial effect on the nanocomposite microstructure and the hard magnetic properties. On the other hand, the single addition of Cu is not beneficial in refining the  $\alpha\text{-Fe}/\text{Nd}_2\text{Fe}_{14}\text{B}$  nanocomposites (Ping et al., 2000). Since, as previously mentioned, the  $\alpha\text{-Fe}/\text{Nd}_2\text{Fe}_{14}\text{B}$  nanocomposites show a higher coercivity than  $\text{Fe}_3\text{B}/\text{Nd}_2\text{Fe}_{14}\text{B}$ , thus it was worth exploring the effect of Cu and Nb additions to  $\alpha\text{-Fe}/\text{Nd}_2\text{Fe}_{14}\text{B}$  nanocomposites as well.

Refinement of the Nd-Fe-B films microstructure to less than 40 nm for the hard grains is essential to obtain the high coercivity and high-energy product (Miyoshi et al., 2000). A number of specific factors including sample composition, spacer layer material and annealing temperature can affect the structure of the thin films and its magnetic properties (Jiang and O'Shea, 2000). Among the metallic elements which can be added to the ternary Nd-Fe-B system with the aim of enhancing the magnetic properties, Cu and Nb are known to act in the sense of promoting the formation of nucleation sites and decreasing the crystalline grain growth, respectively (Ping et al., 2000). The grain refinement by Nb substitution may be responsible for the increase of coercivity,  $H_c$ , and remanence,  $M_r$ .

In this context, results concerning the influence of the composition and thickness of the Nb-Cu spacer layer on the microstructure and magnetic properties of multilayer  $[\text{NdFeB}/\text{NbCu}]_x\text{n}$  films are presented in the following (a-Chiriac et al., 2007). A comparison between the microstructure and magnetic characteristics of Nd-Fe-B, Nd-Fe-B-Nb-Cu and  $[\text{NdFeB}/\text{NbCu}]_x\text{n}$  and thin films is also presented.

The coercivity,  $H_c$ , is an extrinsic magnetic property which is not only influenced by the chemical composition, substrate temperature and crystalline anisotropy, but also depends on the microstructure that is significantly influenced by the deposition and annealing processes.

The XRD analysis revealed that the Nd-Fe-B and  $[\text{NdFeB}/\text{NbCu}]_x\text{n}$  samples in as-deposited state and after thermal standard treatment at temperatures below 550°C, have an amorphous structure. After annealing between 550 and 750°C, the Nd-Fe-B and  $[\text{NdFeB}/\text{NbCu}]_x\text{n}$  thin films undergo a transition from amorphous to crystalline structure and the main diffraction peaks are identified as corresponding to  $\text{Nd}_2\text{Fe}_{14}\text{B}$  tetragonal phase.

The magnetic measurements showed that for low annealing temperatures between 500 and 600°C, the films have an increased value of remanence ratio ( $M_r/M_s = 0.7$ ) and a reduced coercivity due to exchange-coupling interaction between the  $\text{Nd}_2\text{Fe}_{14}\text{B}$  grains. For annealing temperatures over 610°C, for different periods of time, the grains reach sizes between 40 and 60 nm and some Nb- and Cu-secondary phases appear. For these annealed samples the values of the coercive field,  $H_c$ , and the remanence ratio,  $M_r/M_s$ , increase.

Figure 1 shows the dependence of the magnetic properties on the annealing time for annealed  $\text{NbCu}(20\text{nm})/[\text{NdFeB}(180\text{nm})/\text{NbCu}(5\text{nm})]_3/\text{NbCu}(20\text{nm})$  thin film annealed at 610°C.

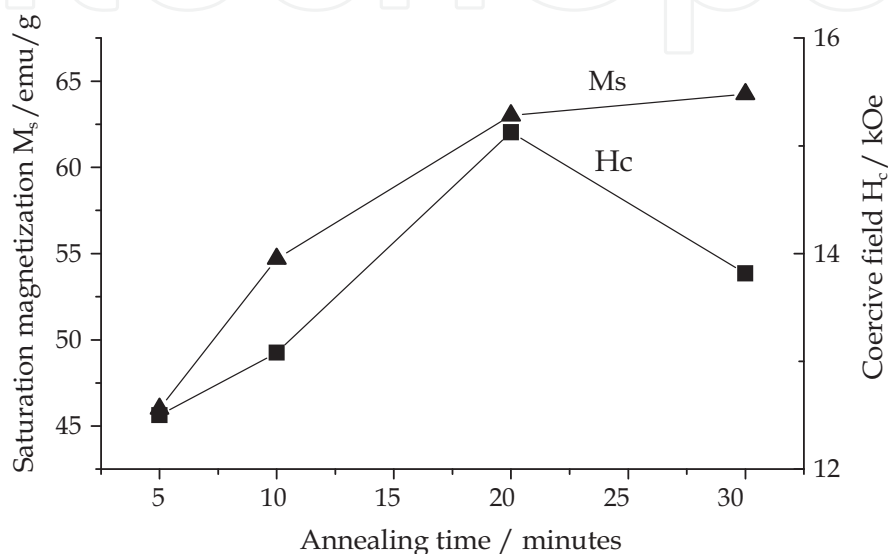


Fig. 1. The dependence of the magnetic properties on the annealing time for multilayer  $\text{NbCu}(20\text{nm})/[\text{NdFeB}(180\text{nm})/\text{NbCu}(5\text{nm})]_3/\text{NbCu}(20\text{nm})$  thin films.

The annealing time below 20 minutes are not enough to promote full crystallization, while time above 20 minutes lead to excessive grain growth. The optimal annealing time was 20 minutes.

Table 1 shows the evolution of main magnetic characteristics of the  $\text{NbCu}(20\text{nm})/[\text{NdFeB}(t_1)/\text{NbCu}]_n/\text{NbCu}(20\text{nm})$  films as a function of different thickness ( $t_1$ ) for Nd-Fe-B layers, after annealing for 20 minutes at different temperatures ( $T_a$ ). The thickness of the Nb-Cu spacer layer is constantly maintained at about 5 nm. The optimal Nd-Fe-B layer thickness was 180 nm.

In Table 1 can be observed that for  $\text{NbCu}/[\text{NdFeB}(180\text{nm})/\text{NbCu}(5\text{nm})]_3/\text{NbCu}$  sample annealed at temperatures  $T_a$  between 610 and 650°C, the coercive field,  $H_c$ , increases from 15.1 kOe to 17 kOe due to the domain wall pinning effect by the Nb- and Cu-based precipitated fine grains, and the saturation magnetization,  $M_s$ , also increases from 63 emu/g to 65 emu/g due to the crystalline structure improvement.

The better hard magnetic characteristics are obtained for  $\text{NbCu}/[\text{NdFeB}(180\text{nm})/\text{NbCu}(5\text{nm})]_3/\text{NbCu}$  film annealed for 20 minutes at 650°C.

In Table 2, the comparative results concerning the hard magnetic characteristics for single layer  $\text{NbCu}(20\text{nm})/\text{NdFeB}(540\text{nm})/\text{NbCu}(20\text{nm})$  and multilayer  $\text{NbCu}(20\text{nm})/[\text{NdFeB}(180\text{nm})/\text{NbCu}(t_2)]_3/\text{NbCu}(20\text{nm})$  film with different thickness ( $t_2$ ) of Nb-Cu spacer layer, after annealing for 20 minutes at 650°C, are presented.

Samples / (all the thicknesses in nm)	M <sub>s</sub> (emu/g)			H <sub>c</sub> (kOe)		
	T <sub>a</sub> (°C)			T <sub>a</sub> (°C)		
	610	650	670	610	650	670
NbCu/NdFeB(540)/NbCu	78.0	98.0	100.0	11.6	12.0	12.4
NbCu/[NdFeB(270)/NbCu(5)]x2/NbCu	76.0	97.0	99.0	12.3	12.8	11.8
NbCu/[NdFeB(180)/NbCu(5)]x3/NbCu	63.0	65.0	70.0	15.1	17.0	13.8
NbCu/[NdFeB(90)/NbCu(5)]x6/NbCu	58.5	59.2	60.1	12.8	15.3	13.2

Table 1. The main magnetic characteristics of the NbCu(20nm)/[NdFeB(t<sub>1</sub>)/NbCu]x<sub>n</sub>/NbCu(20nm) films with different thickness for Nd-Fe-B layers, after annealing at different temperatures for 20 minutes.

Sample / (all the thicknesses in nm)	M <sub>s</sub> (emu/g)	H <sub>c</sub> (kOe)	M <sub>r</sub> /M <sub>s</sub>
NbCu/NdFeB(540)/NbCu	98.0	12.0	0.60
NbCu/[NdFeB(180)/NbCu(3)]x3/NbCu	67.5	19.0	0.80
NbCu/[NdFeB(180)/NbCu(5)]x3/NbCu	65.0	17.0	0.50
NbCu/[NdFeB(180)/NbCu(6)]x3/NbCu	56.0	12.0	0.40
NbCu/[NdFeB(180)/NbCu(10)]x3/NbCu	44.0	11.6	0.44

Table 2. The magnetic characteristics of the NbCu(20nm)/NdFeB(540nm)/NbCu(20nm) film and multilayer NbCu(20nm)/[NdFeB(180nm)/NbCu(t<sub>2</sub>)]x3/NbCu(20nm) film.

It can be observed that the better magnetic properties were obtained for a structure having n = 3 (NdFeB/NbCu) bilayers and a thickness of about 3 nm for the Nb-Cu thin film.

Figure 2 shows the electron micrographs for Nd-Fe-B film (Fig.2a) with the thickness of about 54 nm and NbCu(3nm)/NdFeB(54nm)/NbCu(3nm) film (Fig.2b) with a total thickness of about 60 nm, after annealing under vacuum, for 20 minutes at 650°C.

The micrograph of NbCu(3nm)/NdFeB(54nm)/NbCu(3nm) film presented in Fig. 2b reveals a definite and fine structure of Nd<sub>2</sub>Fe<sub>14</sub>B crystalline grains with dimensions of about 35 nm, as compared to grain sizes of Nd-Fe-B film (Fig. 2a) which are of about 60 nm.

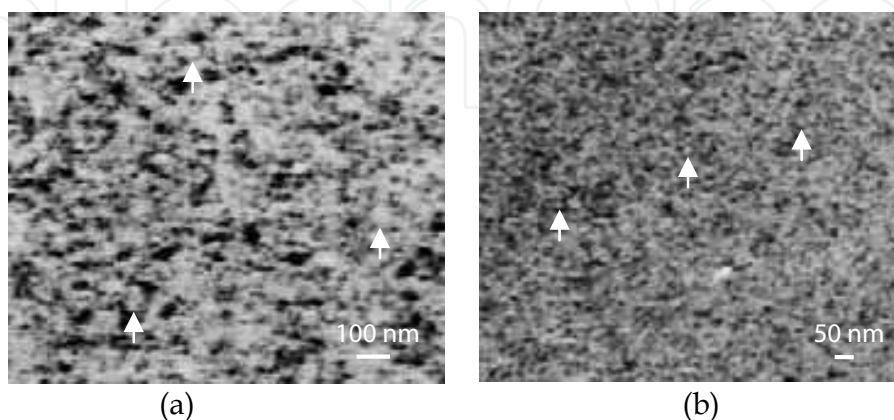


Fig. 2. TEM micrographs of Nd-Fe-B film (a) and NbCu(3nm)/NdFeB(54nm)/NbCu(3nm) film (b), after annealing for 20 minutes at 650°C.

From XRD results, the average dimension of the crystalline grains for NbCu(20nm)/NdFeB(540nm)/NbCu(20nm) sample annealed for 20 minutes at 650°C, is about 40 nm, and this large value is due to the larger thickness of Nd-Fe-B layer of about 540 nm.

Analyzing the presented results it can be observed that, the hard magnetic properties of multilayer [NdFeB/NbCu] $\times$ n thin films sensitively depend on the composition and thickness of the Nb-Cu spacer layer.

As compared to Nd-Fe-B single layer, the multilayer NbCu/[NdFeB(180nm)/NbCu(3nm)] $\times$ n thin films with the thickness of the Nd-Fe-B layer of 180 nm and the thickness of the Nb-Cu layer of about 3 nm exhibit better hard magnetic characteristics such as, coercive force of about 19 kOe and remanence ratio of about 0.8.

Next, some results concerning the Nd-Fe-B with Ta as buffer and capping layers and Nb-Cu additive directly embedded in thin film volume are presented. For Ta/Nd-Fe-B-Nb-Cu/Ta films, the optimum hard magnetic properties have been obtained for following composition determined by SEM/EDS technique: Fe, 64.57 at.%, Cu, 1.81 at.%; Nb, 5.08 at.%; Nd, 13.21 at.%; Ta, 9.43 at.%; and B, up to 100 at.%. For this composition, the 'architecture' of the sputtering composite target is following: disk of Nd<sub>12</sub>Fe<sub>82</sub>B<sub>6</sub> alloy having on its surface chips with the areas of 4.9 cm<sup>2</sup> of Nd, 5.3 cm<sup>2</sup> of B, 4 cm<sup>2</sup> of Nb, and 1.1 cm<sup>2</sup> of Cu.

Table 3 shows the magnetic characteristics of the Ta(40nm)/NdFeBNbCu(540nm)/Ta(20nm) thin films annealed at different temperatures for 20 minutes.

Sample (all the thicknesses in nm)	T <sub>a</sub> (°C)	H <sub>c</sub> (kOe)	M <sub>r</sub> (emu/g)
Ta(40)/NdFeBNbCu(540)/Ta(20)	610	21.7	77.0
	630	22.1	84.5
	650	24.2	82.4
	680	24.0	53.5

Table 3. The magnetic characteristics of the Ta/NdFeBNbCu(540nm)/Ta thin films annealed at different temperatures for 20 minutes.

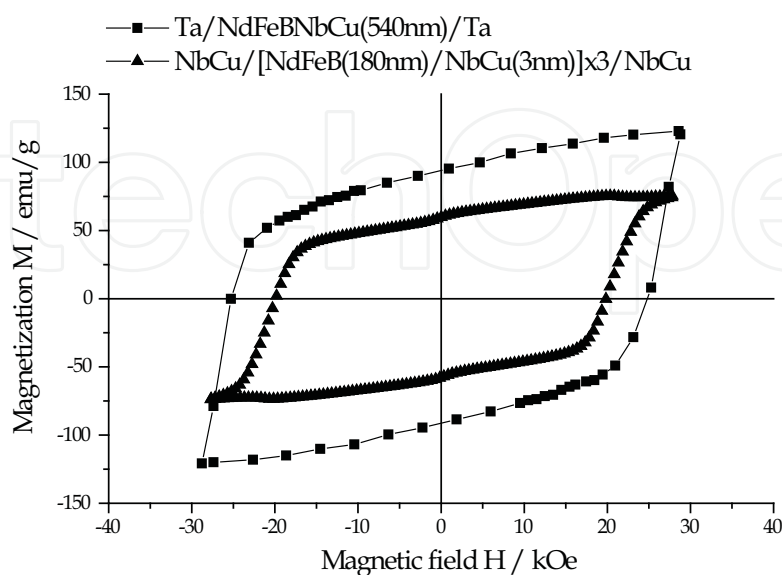


Fig. 3. The hysteresis loops for the Ta/NdFeBNbCu(540nm)/Ta, and multilayer NbCu/[NdFeB(180 nm)/NbCu(3nm)] $\times$ 3/NbCu films annealed for 20 minutes at 650°C.

Annealing between 610 and 630°C leads to an increase of the remanent magnetization,  $M_r$ , values from 77 to 84.5 emu/g due to the exchange-coupling effect between the  $\text{Nd}_2\text{Fe}_{14}\text{B}$  grains. For samples annealed at these temperatures the coercive field value slightly increases. The better hard magnetic characteristics are obtained for samples annealed for 20 minutes at 650°C.

In Figure 3, the hysteresis loops for the Ta(40nm)/NdFeBNbCu(540nm)/Ta(20nm) single layer and multilayer NbCu(20nm)/[NdFeB(180nm)/NbCu(3nm)] $\times$ 3/NbCu(20nm) thin film, annealed for 20 minutes at 650°C are comparatively presented. It can be observed that the use of Ta films as buffer and capping layers and of Nb-Cu additive directly embedded in the film volume during deposition by sputtering composite targets is very effective in enhancing the coercive field,  $H_c$ , and saturation magnetization of Ta(40nm)/NdFeBNbCu(540nm)/Ta(20nm) samples.

#### 4.2 Influence of Co addition

Addition of cobalt (Co) to  $\text{Nd}_2\text{Fe}_{14}\text{B}$  nanocomposite magnets results in an increase of the Curie temperature and can result in an improvement of hard magnetic properties. Small Co addition leads also to a small increase in magnetization (Matsuura et al., 1985). In (Nd,Pr)-(Fe,Co)-B alloys, a Co content of about 30% improves the thermal stability through enhanced Curie temperature but it may decrease the coercivity (Harland and Davies, 2000).

Results concerning the influence of the simultaneous Nb-Cu and Co additions and the stratification effect on the microstructure and hard magnetic properties of multilayer Ta/[NdFeBNbCu/Co] $\times$ n/Ta thin films (b-Chiriac et al., 2007) are described below.

In Figure 4 the dependence of the coercive field,  $H_c$ , and saturation magnetization,  $M_s$ , on the thickness of the Co layers for multilayer Ta/[NdFeBNbCu(180nm)/Co( $t$ ) $\times$ 3/Ta thin films annealed for 20 minutes at 650°C is presented.

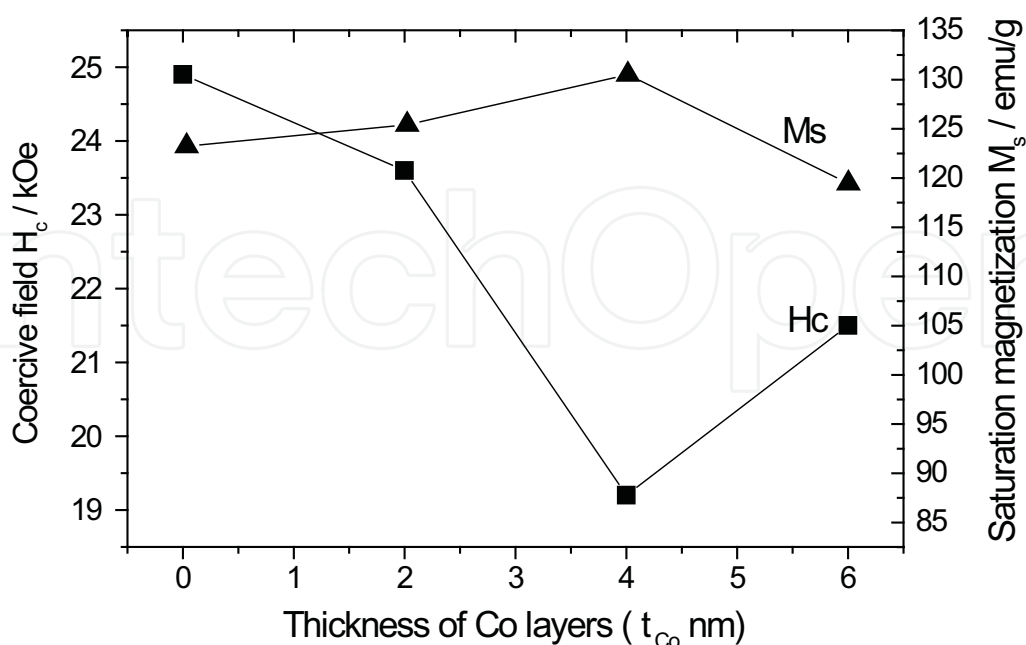


Fig. 4. The dependence of the hysteresis parameters on the thickness of the Co layers for Ta/[NdFeBNbCu (180 nm)/Co( $t$  nm)] $\times$ 3/Ta films annealed for 20 minutes at 650°C.

The coercive field,  $H_c$ , decreases for thicknesses of the Co layers of up to 4 nm, since the Co phase has a much lower anisotropy than  $\text{Nd}_2\text{Fe}_{14}\text{B}$  phase and the average anisotropy of the coupled phases is decreased (Cui and O'Shea, 2004). For larger Co thickness, the coercive field presents an inexplicable increase up to 6 nm, reason for which an extended research effort is needed. It can be also observed that there is a gradual increase of the saturation magnetization with the increase of the thickness of the Co layers up to 4 nm, followed by a slow decrease for Co layers with the thickness of 6 nm. A similar behavior for the dependence of the saturation magnetization on the Co content was noticed in Nd-Fe-Co-B quaternary alloys,  $\text{R}_2(\text{Fe}_{1-x}\text{Co}_x)_{17}$  pseudobinary systems, and  $\text{Fe}_{1-x}\text{Co}_x$  binary systems (Matsuura et al., 1985). When Co substitutes Fe, the saturation magnetization increases slightly to a maximum (i.e.,  $x = 0.1$  for  $\text{Nd}_2(\text{Fe}_{1-x}\text{Co}_x)_{14}\text{B}$  and  $x = 0.4$  for  $\text{R}_2(\text{Fe}_{1-x}\text{Co}_x)_{17}$ ) and subsequently decreases for larger Co contents. For Ta/[NdFeBNbCu(180nm)/Co(t)]x3/Ta structure when the thickness of the Co layer is 4 nm, Co represents about 2.8% from the total volume of multilayer [NdFeBNbCu(180nm)/Co(4nm)]x3 system, which is the optimum content for the highest saturation magnetization. When the thickness of the Co layer is of 6 nm, the Co content from [NdFeBNbCu(180nm)/Co(6nm)]x3 system represents about 4.25%, and in this case the saturation magnetization decreases.

Table 4 compares the magnetic characteristics for Ta/[NdFeBNbCu(t)/Co(2nm)]xn/Ta system with different thickness (t) of NdFeBNbCu layers, annealed at different temperatures for 20 minutes.

Samples (all the thicknesses in nm)	$T_a$ (°C)	$H_c$ (kOe)	$M_r$ (emu/g)
Ta/[NdFeBNbCu(270)/Co(2)]x2/Ta	610	23.2	69.6
	630	22.9	70.6
	650	20.1	70.6
	680	23.9	71.7
	700	23.5	84.5
Ta/[NdFeBNbCu(180)/Co(2)]x3/Ta	610	18.4	100.6
	630	18.7	94.2
	650	22.7	100.6
	680	22.5	79.2
	700	20.2	91.0
Ta/[NdFeBNbCu(90)/Co(2)]x6/Ta	610	13.0	94.2
	650	8.8	82.4
	680	13.1	75.0
	700	9.5	101.7

Table 4. The magnetic properties for Ta/[NdFeBNbCu(t)/Co(2nm)]xn/Ta system with different thickness of NdFeBNbCu layers annealed at different temperatures for 20 minutes.

It can be observed that Ta/[NdFeBNbCu(180nm)/Co(2nm)]x3/Ta films annealed at 650°C for 20 minutes, present the optimum hard magnetic properties for practical applications such as thin-film permanent magnets.

Figure 5 shows the thermomagnetic curves of the magnetic Ta/NdFeBNbCu(540nm)/Ta single layer and multilayer Ta/[NdFeBNbCu(180nm)/Co(2nm)]x3/Ta films after devitrification and crystallization treatments at 650°C for 20 minutes.

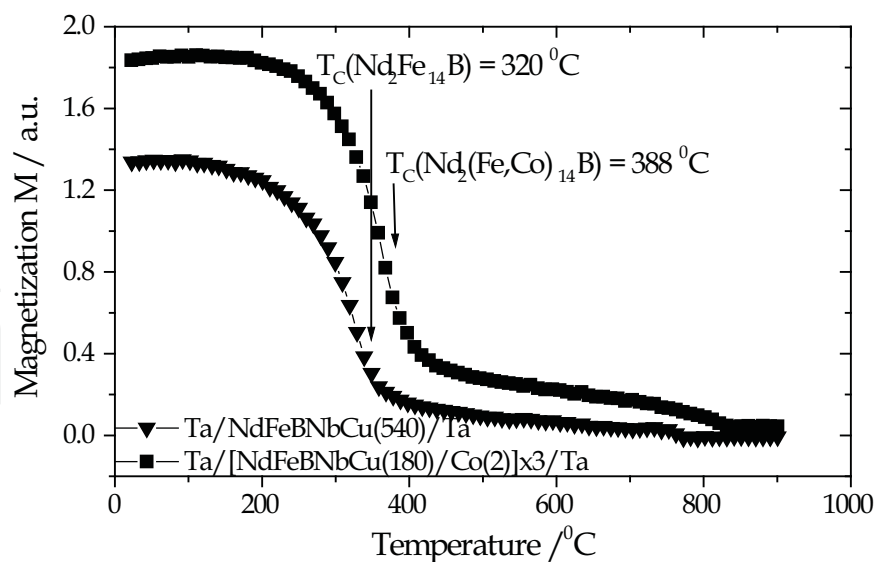


Fig. 5. The thermomagnetic curves of the Ta/NdFeBNbCu(540nm)/Ta and Ta/(NdFeBNbCu(180nm)/Co(2nm)]x3/Ta thin films, annealed at 650°C for 20 minutes.

From thermomagnetic curves, it can be observed that the multilayer Ta/[NdFeBNbCu(180nm)/Co(2nm)]x3/Ta thin film presents an increase in the Curie temperature,  $T_c$ , of about 68°C, as compared to Ta/NdFeBNbCu(540 nm)/Ta magnetic single layer.

#### 4.3 Influence of Si addition

The addition of small amounts of Si to Nd-Fe-B system was reported to result in an increase in the Curie temperature,  $T_c$ , of the Nd<sub>2</sub>Fe<sub>14</sub>B phase, improvement of the intrinsic coercive field,  $H_c$ , of the nanocomposite magnets (Cui et al., 2000) and more rectangular hysteresis loops (Coey, 1996).

The influence of Nd-Fe-B-Nb-Cu film stratification and thermal treatments on the hard magnetic properties and microstructure of multilayer [NdFeBNbCu/FeBSi]<sub>xn</sub> thin films was recently studied (Chiriac et al., 2008). For multilayer [NdFeBNbCu/FeBSi]<sub>xn</sub> films, the thickness of Nd-Fe-B-Nb-Cu layers was varied from 30 to 540 nm and the thickness of the Fe-B-Si spacer layer was varied from 2.5 to 20 nm. The total thickness of Nd-Fe-B-Nb-Cu layers was 540 nm.

The composition of Fe-B-Si film obtained by SEM/EDS technique is as follows: Fe 70 at.%; Si 15 at.%; B up to 100 at.%.

During the annealing process, the elements within the Ta/[NdFeBNbCu/FeBSi]<sub>xn</sub>/Ta multilayer films diffuse and a mixture consisting of hard magnetic and soft magnetic phases is created in different ratios depending on the thicknesses of the constituent layers and annealing temperature. The X-ray diffraction investigations indicated that Ta/[NdFeBNbCu/FeBSi]<sub>xn</sub>/Ta thin films, in as-deposited state and after thermal treatments at temperatures below 570°C, have amorphous structure. At annealing temperatures between 570 and 600°C, the microstructure of the samples consists of a small number of Fe<sub>3</sub>B nanograins, which are embedded in the amorphous matrix. Samples annealed at temperatures higher than 650°C exhibit a complex multiphase structure of tens of nanometers.

Figure 7 shows the X-ray diffraction patterns for selected samples in as-deposited state and after annealing at specific optimum temperatures as follows: Ta/NdFeBNbCu(540nm)/Ta single layer in as-deposited state, curve (a) and after annealing at temperature of 650°C for

20 minutes, curve (b), and multilayer Ta/[NdFeBNbCu(180nm)/FeBSi(15nm)]x3/Ta films after annealing at 680°C for 20 minutes, curve (c).

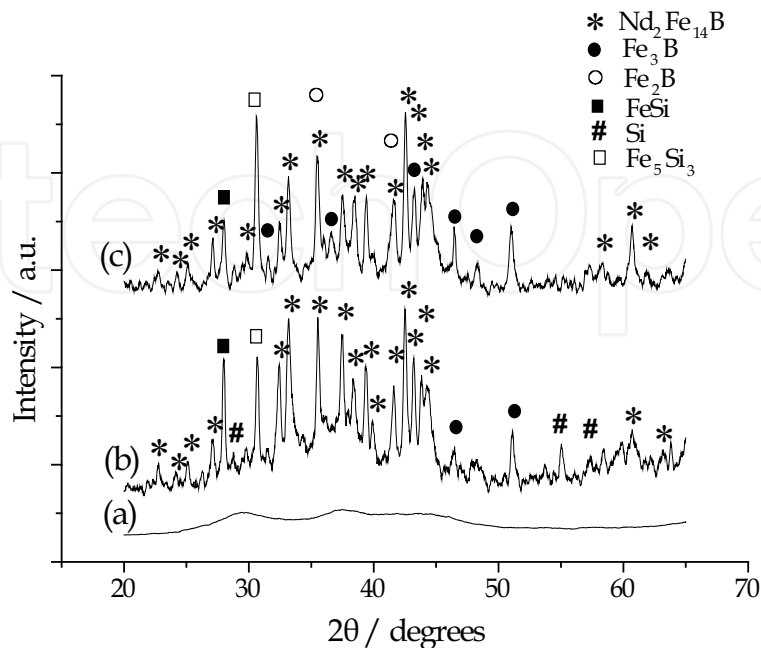


Fig. 7. X-ray diffraction patterns of the Ta/NdFeBNbCu(540nm)/Ta single layer in as-deposited state and after annealing at 650°C for 20 minutes (curves a and b), and multilayer Ta/[NdFeBNbCu(180nm)/FeBSi(15nm)]x3/Ta films after annealing at temperature of 680°C for 20 minutes (curve c).

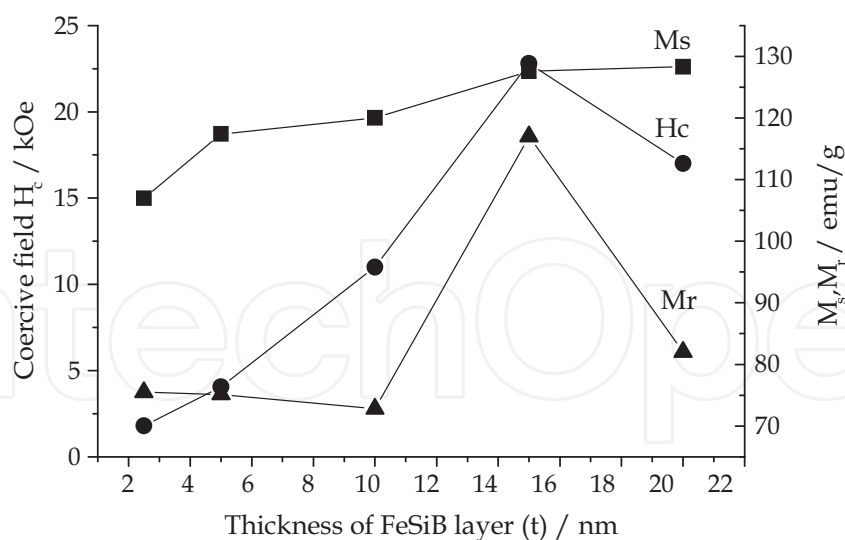


Fig. 8. The dependence of the magnetic parameters on the thickness (t) of the Fe-B-Si layers for multilayer Ta/[NdFeBNbCu(180nm)/FeBSi(t)]x3/Ta films annealed at 680°C for 20 minutes.

It can be observed that the as-deposited Ta/NdFeBNbCu(540 nm)/Ta single layer has an amorphous structure. After annealing, the Ta/[NdFeBNbCu(180nm)/FeBSi(15nm)]x3/Ta multilayer film presents a multiphase structure consisting of a mixture of nanograins of

$\text{Nd}_2\text{Fe}_{14}\text{B}$  hard magnetic phase and  $\text{Fe}_3\text{B}$ ,  $\text{Fe}_{23}\text{B}_6$ ,  $\text{Fe}_2\text{B}$ ,  $\text{FeSi}$ , and  $\text{Fe}_5\text{Si}_3$  soft magnetic phases (curve c). For the Ta/NdFeBNbCu/Ta single layer annealed at  $650^\circ\text{C}$  for 20 minutes, curve (b), the average crystalline size of  $\text{Nd}_2\text{Fe}_{14}\text{B}$  phase is about 35 nm, while for Ta/[NdFeBNbCu(180nm)/FeBSi(15nm)]x3/Ta multilayer film annealed at  $680^\circ\text{C}$  for 20 minutes, curve (c), is about 30 nm. The average crystalline size of soft magnetic phases is about 10 nm. In Figure 8, the dependence of the coercive field,  $H_c$ , saturation magnetization,  $M_s$ , and remanent magnetization,  $M_r$ , on the thickness ( $t$ ) of the Fe-B-Si layers for Ta/[NdFeBNbCu(180nm)/FeBSi(15nm)]x3/Ta multilayer films annealed at  $680^\circ\text{C}$  for 20 minutes is presented.

It can be observed that the highest values of coercive field, saturation magnetization, and remanence are simultaneously reached when the thickness of the Fe-B-Si layers increases up to 15 nm. A decrease in coercive field and remanence was noticed when the thickness of Fe-Si-B layer was increased to 20 nm.

Typical magnetic hysteresis loops for Ta/[NdFeBNbCu(180nm)/FeBSi(15nm)]x3/Ta multilayer thin films annealed at different temperatures between  $630$  and  $700^\circ\text{C}$  for 20 minutes are shown in Figure 9.

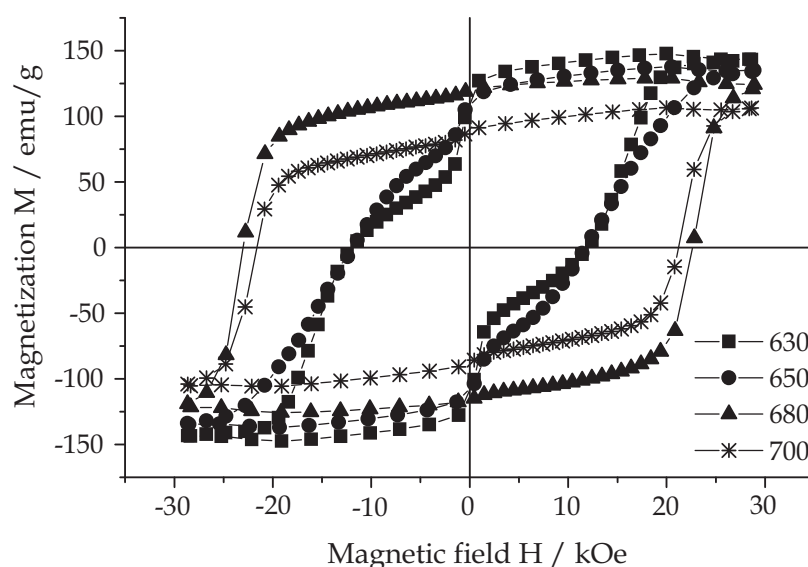


Fig. 9. Room-temperature hysteresis loops of multilayer Ta/[NdFeBNbCu(180nm)/FeBSi(15 nm)]x3/Ta thin film annealed at different temperatures between  $630$  and  $700^\circ\text{C}$ .

It can be observed that the optimum magnetic parameters are obtained for the sample annealed at  $680^\circ\text{C}$  for 20 minutes. An obvious 'shoulder' on the hysteresis loops of the samples annealed at  $630$  and  $650^\circ\text{C}$  is observed, due to weak exchange coupling between the soft and hard phases.

In Figure 10, the hysteresis loops for Ta/NdFeBNbCu(540nm)/Ta single layer and Ta/[NdFeBNbCu(180nm)/FeBSi(15 nm)]x3/Ta thin film are comparatively presented.

One can observe that the stratification effect by using Fe-B-Si film as spacer layer has an influence on the rectangular aspect of the hysteresis loop of the Ta/[NdFeBNbCu(180nm)/FeBSi(15nm)]x3/Ta thin film as compared to the hysteresis loop of the Ta/NdFeBNbCu(540 nm)/Ta thin film.

The thermomagnetic measurements indicate that the Fe-B-Si spacer layer in multilayer Ta/[NdFeBNbCu(180nm)/FeBSi( $t$ )]x3/Ta thin film results in an increase of the Curie

temperature. The thermomagnetic measurements for multilayer Ta/[NdFeBNbCu(180nm)/FeBSi(15nm)]x3/Ta thin film annealed at 680°C for 20 minutes reveal an average increase in the Curie temperature of about 17°C, as compared to Ta/NdFeBNbCu(540nm)/Ta film.

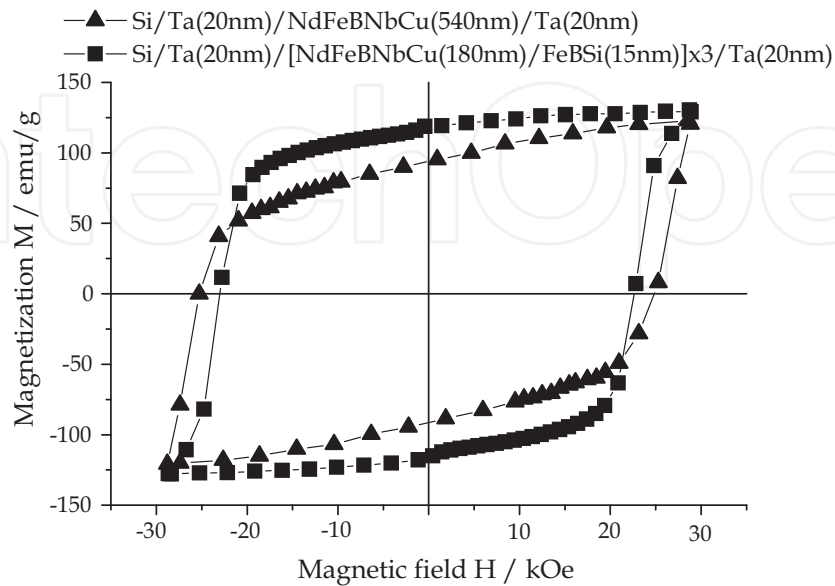


Fig. 10. Room-temperature hysteresis loops of Ta/NdFeBNbCu(540 nm)/Ta single layer and multilayer Ta/[NdFeBNbCu(180nm)/FeBSi(15 nm)]x3/Ta thin film.

#### 4.4 Influence of other additives

In Nd-Fe-B samples, the substitution of Nd by Dy increases the magnetocrystalline anisotropy of the  $\text{Nd}_2\text{Fe}_{14}\text{B}$  phase, giving rise to an improved coercive field without a significant loss in remanent magnetization (Kanekiyo and Hirosawa, 1998). By increasing Nd content from 14 to 20-30%, crystallization temperature of the hard phase decreases from 575°C to 500°C (Van Khoa et al., 2006).

The addition of 1.1 at. % Mo, Si or Ga to Nd-Fe-B system results in an increase in the Curie temperature,  $T_c$ , of the hard phases and the improvement of the intrinsic coercivity of the nanocomposite magnets (Cui et al., 2000).

Van Khoa and co-workers (2008) studied the effect of the thickness ( $d$ ) of the Fe buffer layers on the Curie temperature and the remanent magnetization of the multilayer Si/Mo(20nm)/[NdFeB(35nm)/Fe( $d$ (Fe))]/Mo(30nm)( $d$ (Fe)) films. The Curie temperature and remanent magnetization of the films increased when thickness of Fe layer was increased from 0 to 10 nm and was decreased when thickness of Fe layer reached 15 nm.

The replacement of a Fe-based soft phase by a semihard phase (i.e.  $\text{Fe}_{1-x}\text{Co}_x$  alloys) yields a trivial improvement of the coercive field because the average anisotropy ( $K_1$ ) increases. The  $\text{Fe}_{1-x}\text{Co}_x$  alloys are ideal candidates for the hard-soft permanent magnet nanostructuring because they have a very high magnetization in a wide range of Fe-rich compositions, 24.3 kG in  $\text{Fe}_{65}\text{Co}_{35}$  (Skomski et al., 2009; Ao et al., 2006).

Wang and co-workers (2007) show that the addition of Zr can prevent the formation of  $\text{Nd}_3\text{Fe}_{62}\text{B}_{14}$  metastable phase and refine the grain sizes of  $\alpha$ -Fe and  $\text{Nd}_2\text{Fe}_{14}\text{B}$  phases, thus improving the magnetic properties, especially the coercive field of nanocomposite hard magnetic materials. The crystallization behavior changes from a two-step process to a

single-step process, and  $\text{Nd}_2\text{Fe}_{14}\text{B}$  and  $\alpha\text{-Fe}$  precipitate simultaneously from the amorphous phase. The addition of Zr is also advantageous in improving the energy product and squareness of hysteresis loops in  $\text{Nd}_2\text{Fe}_{14}\text{B}/\alpha\text{-Fe}$  nanocomposites (Chang et al., 1999). Moreover, Jurczyk and Wallace (1986) reported that insertion of a proper amount of Zr in  $\text{Nd}_2\text{Fe}_{14}\text{B}$  phase may increase the anisotropy field of the alloy, and accordingly,  $H_c$  is remarkably increased, along with the magnetic energy product. The entrance of Zr element into  $\text{Nd}_2\text{Fe}_{14}\text{B}$  unit cell may slightly decrease the Curie temperature  $T_c$  of  $\text{Nd}_2\text{Fe}_{14}\text{B}$  phase.

## 5. Exchange coupling

It is well known that the good permanent magnetic properties of Nd-Fe-B nanocomposite magnets are generated through the magnetic hardening of the iron based soft magnetic phases (i.e.  $\alpha\text{-Fe}$ ,  $\text{Fe}_3\text{B}$ ,  $\text{Fe}_{23}\text{B}_6$ ) by the  $\text{Nd}_2\text{Fe}_{14}\text{B}$  hard magnetic phase. This occurs when the structure is homogeneous and refined to the nanometer scale, thus ensuring effective magnetic coupling of the grains over short distances through exchange interactions (Kneller and Hawing, 1991). Decreased grain size that leads to a stronger interface exchange coupling between grains (Cui and O'Shea 2003).

The appropriate refinement of the soft grains is favorable for the exchange fields from the nearest grains of the hard phase to fully cover the soft grain embedded between the hard grains and suppress the easy nucleation of inverse magnetization in the soft grain. On the other hand, the refinement of both the soft and hard grains results in a significantly increasing ratio of the interface area (or grain boundary area) to the volume of the grains. With an increasing percentage of grain interfaces or grain boundaries, the obstacles to propagation of inverse magnetization grow in number. Because the probability of the direct contact between the soft and the hard grains increases, the exchange coupling between the soft grain and the hard grains nearest in proximity is enhanced and plays an essential role in determining the magnetic properties of the nanocomposite magnets (Cui et al., 2000).

Exchange interactions between neighboring soft and hard grains lead to remanence enhancement of isotropically oriented grains in nanocrystalline composite magnets (Fidler and Schrefl, 2000). The magnetic properties of the samples decrease with the coarsening of the hard grains. The larger the hard grains the smaller probability of the direct contact between the soft and hard grains. Thus, for nanocomposite hard magnetic samples, the exchange coupling between the soft grain and its nearest hard grains is weakened. Thus, the magnetic properties of the nanocomposite magnets are deteriorated (Cui et al., 2000).

Too large or too small a grain size of  $\alpha\text{-Fe}$  is unfavorable for the improvement of the magnetic properties of the nanocomposite hard magnetic samples. A  $\alpha\text{-Fe}$  grain with a large grain size cannot be fully penetrated by the exchange fields coming from the hard magnetic grains nearest in proximity, due to the short-range feature of the exchange interaction. In this case, the nucleation of the reverse magnetization can be easily produced at the middle of the  $\alpha\text{-Fe}$  grains, where it is free from the exchange fields. Obviously, this is harmful to the permanent magnetic properties. The too small  $\alpha\text{-Fe}$  grains are always attained at a relatively low crystallization temperature at which the incomplete formation of the hard phase is obviously unfavorable for the magnetic properties of nanocomposite magnets (Cui et al., 2000).

The results obtained by Fukunaga and co-workers (1999) confirm the increase of coercivity owing to reduced intergrain exchange interactions, provided that grain size is sufficiently small. At the same time, small grain size of the hard phase facilitates the exchange coupling

between grains, thus increasing the remanence. The authors proposed a two-phase microstructure consisting of Nd-Fe-B and  $\alpha$ -Fe grains embedded within a residual amorphous phase. The amorphous intergranular phase is expected to reduce the exchange interactions between the hard and the soft grains, leading to an improved coercive field.

To obtain a more ideal structure with a uniform distribution of the soft and hard phases, a multilayered structure is a best appropriate way. Non-uniform clustering of  $\alpha$ -Fe after annealing is not favorable for exchange coupling between the hard and soft phases, resulting in poor permanent-magnetic properties in the nanocomposite single layer (Liu et al., 2003).

The results concerning the magnetic interactions within the multilayer Ta/[NdFeBNbCu/FeBSi] $\times$ 3/Ta thin films are presented in the following, based on some recent reports (Chiriac et al., 2008). The refinement of the grain sizes by a controlled thermal treatment was used to enhance the exchange coupling between the hard and soft magnetic grains in multilayer Ta/[NdFeBNbCu(180nm)/FeBSi(15nm)] $\times$ 3/Ta thin films.

The  $\delta M$  versus H measurements are used to verify the nature of exchange coupling between the hard and soft magnetic phases in nanocomposite magnets. The  $\delta M$  is defined as  $m_d(H) - [1 - 2m_r(H)]$ , where  $m_d(H)$  is the reduced demagnetization remanence ( $M_d(H)/M_r$ ) and  $m_r(H)$  is the reduced magnetization remanence ( $M_r(H)/M_r$ ) (Rama Rao et al., 2007). Figure 11 shows the  $\delta M$  plots for Ta/[NdFeBNbCu(180nm)/FeBSi(15nm)] $\times$ 3/Ta thin films after annealing at different temperatures for 20 minutes.

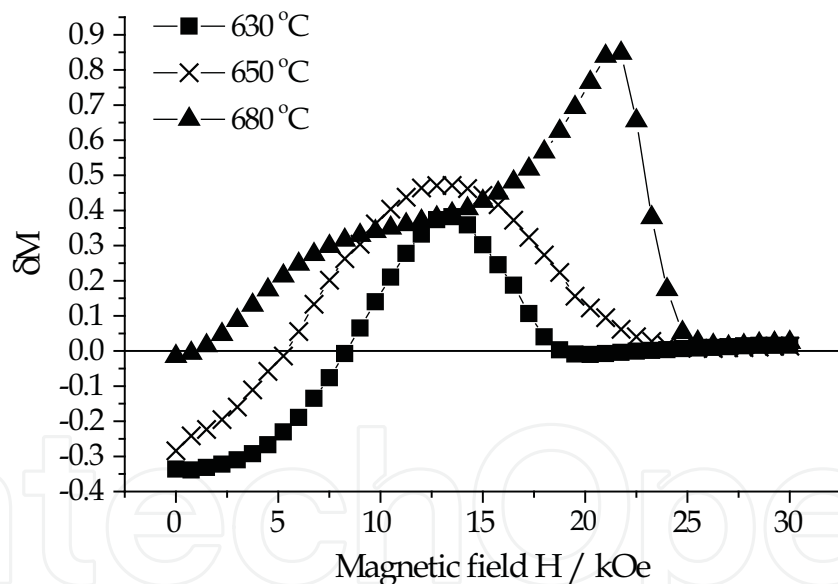


Fig. 11.  $\delta M$  versus applied magnetic field for Ta/[NdFeBNbCu(180nm)/FeBSi(15nm)] $\times$ 3/Ta thin films after annealing at different temperatures for 20 min.

It can be observed an increase in exchange interaction between the soft and hard magnetic grains with the increase of the annealing temperature to 680°C. For samples annealed at 630°C and 650°C an initially negative  $\delta M$ , for magnetic fields between 0 and about 6.8 kG, is observed, indicating the existence of magnetostatic interactions between soft and hard grains. A positive  $\delta M$  is observed afterwards indicating the existence of exchange coupling between soft and hard grains. For Ta/[NdFeBNbCu(180nm)/FeBSi(15nm)] $\times$ 3/Ta thin film, annealing at a temperature increased to 680°C for 20 min., leads to a grain growth resulting in an effective exchange-coupling.

The strength of the coupling / decoupling of soft and hard magnetic grains is determined by variation of specific magnetization ( $\sigma$ ) as a function of applied magnetic field ( $H$ ). The irreversible susceptibilities  $\chi_{irr}$  ( $\chi_{irr} = d\sigma/dH$ ) as a function of the demagnetising fields for Ta/[NdFeBNbCu(180nm)/FeBSi(15nm)]x3/Ta thin films annealed at temperatures between 630°C and 680°C are presented in Figure 12. The main peaks correspond to the nucleation fields for magnetisation reversal. In comparison with the samples annealed at 680°C, for the samples annealed at 630°C and 650°C, non-simultaneous switching of the magnetization in the hard and soft magnetic phases leads to differences between the coercivity,  $H_c$ , and the nucleation field,  $H_n$ .

The two peaks shown in the ( $\chi_{irr}$ ) curve of Figure 12 for the sample annealed at 630°C could be due to the presence of the smaller soft magnetic grains confirmed by an obvious shoulder in II quadrant of the hysteresis loop (Fig.9). From Figures 9 and 12 it can be observed that the Ta/[NdFeBNbCu(180nm)/FeBSi(15nm)]x3/Ta thin films annealed at 680°C for 20 minutes show a hysteresis loop with no constriction and a strong exchange coupling effect between the soft and hard magnetic phases.

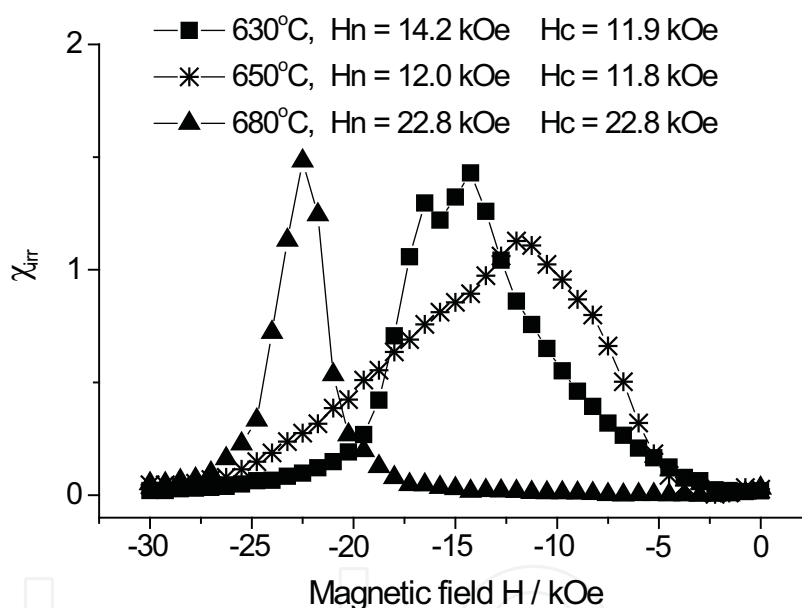


Fig. 12. The irreversible susceptibilities,  $\chi_{irr}$ , as a function of the demagnetising fields for Ta/[NdFeBNbCu(180nm)/FeBSi(15nm)]x3/Ta thin films annealed at temperatures between 630 and 680°C.

## 6. Thermal stability

In order to be used in applications like MEMS devices, and information storage media, the thin film magnets should exhibit specific characteristics: (1) large coercivity, remanent magnetization, saturation magnetization ( $M_s$ ) and energy product  $(BH)_{max}$ ; (2) good thermal stability; (3) adaptability to the specific applications processing. For permanent magnets that have to operate at elevated temperatures the irreversible loss of magnetization, which causes short-time or long-term flux losses, is an important criterion for evaluating the thermal stability (Liu and Davies, 2007).

The thermal stability of permanent magnets can be increased by increasing the Curie temperature and intrinsic coercivity. The increase of the Curie temperature,  $T_c$ , can be achieved by partial substitution of Fe with Co (Liu and Davies, 2007; b-Chiriac et al., 2007). Supplementary, as described in the previous chapter sections, the addition of elements like Nb or/and Cu, Mo and Zr to Nd(Fe,Co)B ternary films is an effective way to improve their hard magnetic properties.

The  $H_c$  and  $M_r$  losses (L) were calculated using following equations (Liu and Davies, 2007):

$$L_{Hc} = \frac{H_{cB}(25^\circ C) - H_{cA}(25^\circ C)}{H_{cB}(25^\circ C)} \times 100\%, \quad L_{Mr} = \frac{M_{rB}(25^\circ C) - M_{rA}(25^\circ C)}{M_{rB}(25^\circ C)} \times 100\%$$

where  $H_{cB}$  and  $M_{rB}$ ,  $H_{cA}$  and  $M_{rA}$  are the room temperature coercivity and remanence, respectively, before (B) and after (A) exposure to an elevated temperature.

Nanocomposite alloys present irreversible losses lower than single phase nanocrystalline alloys, because of the additional exchange coupling and enhancement in  $M_r$  imparted by the presence of soft magnetic phase with a higher saturation magnetization than for the  $Nd_2Fe_{14}B$  hard phase (Liu and Davies, 2007).

Liu and Davies (2007) shown that the Co substitution improves the thermal stability of nanocrystalline (Nd/Pr)-(Fe/Co)-B alloys by reducing the long-term and short-time irreversible losses in coercive field and remanent magnetization as a result of the enhancement in Curie temperature and possibly also because of improved corrosion resistance. The thermal stability evolution of Nd-Fe-B, Nd-Fe-B-Nb-Cu and [NdFeBNbCu/Co] $\times$ 3 thin films as a result of their thermal cycling in the temperature range 25 $\div$ 350 $^\circ$ C is comparatively presented.

The influence of the ageing at 150 $^\circ$ C, for different periods of time, on the losses in  $H_c$  and  $M_r$  was also studied (Chiriac et al., 2009). All the as-deposited thin films were thermally treated in vacuum at 650 $^\circ$ C for 20 min, for their devitrification and crystallization. In our experiments, the thermal stability of crystallized samples was estimated in two ways: (1) S1 sample sets were maintained at constant temperature (150 $^\circ$ C) for different periods of time and the subsequent magnetic measurements were routinely performed after cooling at 25 $^\circ$ C; (2) the magnetic characteristics of S2 sample sets were measured at different temperatures in the range 25 $\div$ 350 $^\circ$ C.

For the Ta/[NdFeBNbCu(540)/Ta thin film, the temperature coefficient of remanent magnetization ( $\alpha$ ) and the temperature coefficient of coercivity ( $\beta$ ) in the temperature range 25 $^\circ$ C $\div$ 150 $^\circ$ C are -0.029%/ $^\circ$ C and -1.02%/ $^\circ$ C, respectively.

Figure 13 shows the demagnetization curves for Ta/[NdFeBNbCu(180nm)/Co(2 nm)] $\times$ 3/Ta thin film at various temperatures between 25 $^\circ$ C and 350 $^\circ$ C. It can be observed that the coercivity and remanence decrease with increasing the temperature up to 350 $^\circ$ C, but they reach the initial value when cooling back to 25 $^\circ$ C.

Based on the data presented in Figure 14,  $\alpha$  and  $\beta$  coefficients in the temperature range 25 $^\circ$ C $\div$ 150 $^\circ$ C for Ta/[NdFeBNbCu(180 nm)/Co(2 nm)] $\times$ 3/Ta thin film are about -0.025%/ $^\circ$ C and -0.39%/ $^\circ$ C, respectively. It can be observed that low values of the  $\alpha$  and  $\beta$  coefficients for Ta/[NdFeBNbCu(180 nm)/Co(2 nm)] $\times$ 3/Ta thin film in the temperature range 25 $^\circ$ C $\div$ 150 $^\circ$ C satisfy the needs of planar permanent magnets as actuator elements for MEMS applications (Walther et al., 2009).

The thermal stability of Ta/NdFeB/Ta, Ta/NdFeBNbCu/Ta and Ta/[NdFeBNbCu/Co] $\times$ n/Ta thin films represented by the losses in  $H_c$  and  $M_r$  has been also investigated. The Ta/NdFeB/Ta, Ta/NdFeBNbCu/Ta and Ta/[NdFeBNbCu/Co] $\times$ n/Ta thin-film magnets (sample set S1) were successively aged at 150°C for different time periods between 5 h and 500 h. For the samples aged for 100 h, the coercivity losses are of 0.8% for Ta/[NdFeBNbCu/Co] $\times$ 3/Ta films, of 0.92% for Ta/[NdFeBNbCu/Ta films and of 1.1% for Ta/NdFeB/Ta films, whereas the remanence magnetization losses are 4.2%, 5.1% and 6.8%, respectively. The ageing of the Nd-Fe-B samples with additions at 150°C for time periods larger than 100 h, has not generated notable changes in coercivity and remanence losses.

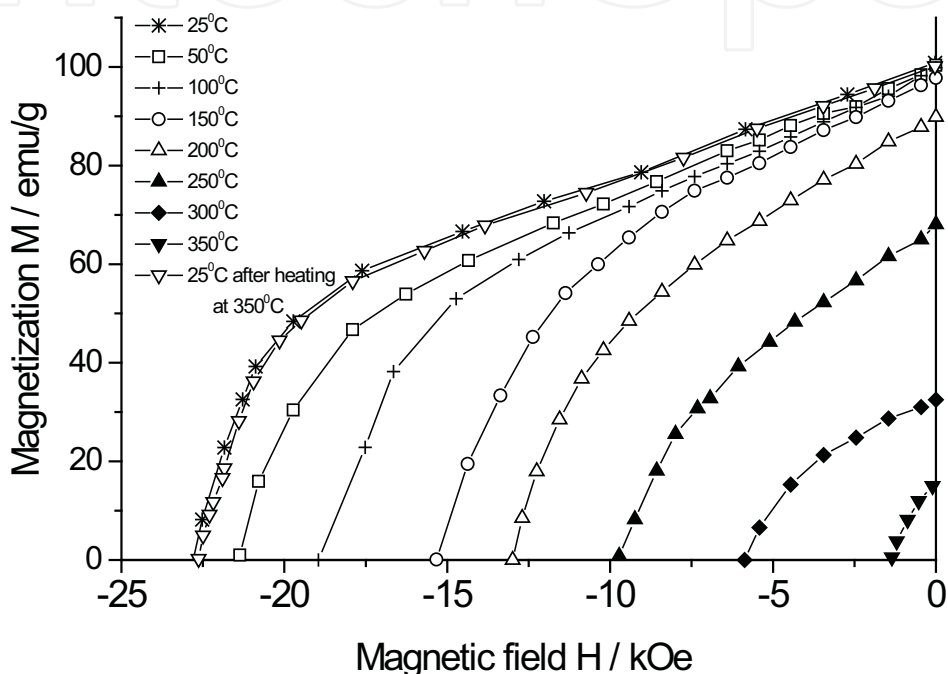


Fig. 13. Demagnetization curves for Ta/[NdFeBNbCu(180nm)/Co(2nm)] $\times$ 3/Ta thin films at various temperatures between 25°C and 350°C.

As compared to the samples aged at 150°C for 100 h, the Co-containing samples aged for 500 h exhibit changes in coercivity and remanence losses lower than 0.2% and 0.5%, respectively.

Figures 14.(a, b) present the evolution of the main magnetic parameters, coercivity (a) and remanence magnetization (b), of the sample set S2 as a function of temperature in the range 25÷150°C.

The results show that the coercivity losses increase with increasing the temperature, but they are reversible, which indicates that these thin films are suitable for high temperature applications.

In Figure 14 b, for all the samples, only small losses in  $M_r$  occurred for temperature up to 150°C, but afterwards the losses increase rapidly, especially for temperature higher than 200°C due to structural changes in the surface and volume of the samples after heating at high temperatures.

As compared to Ta/NdFeB(540)/Ta and Ta/[NdFeBNbCu(540nm)/Ta films, the Ta/[NdFeBNbCu(180nm)/Co(2nm)] $\times$ 3/Ta films with a small Co content (about 1.5% in

total magnetic volume) exhibit  $H_c$  losses of about 26% and  $M_r$  losses of about 4%. This small change in the losses of Ta/[NdFeBNbCu(180)/Co(2)] $\times$ 3/Ta samples is due to the increase in the corrosion resistance and in the Curie temperature with about 68°C.

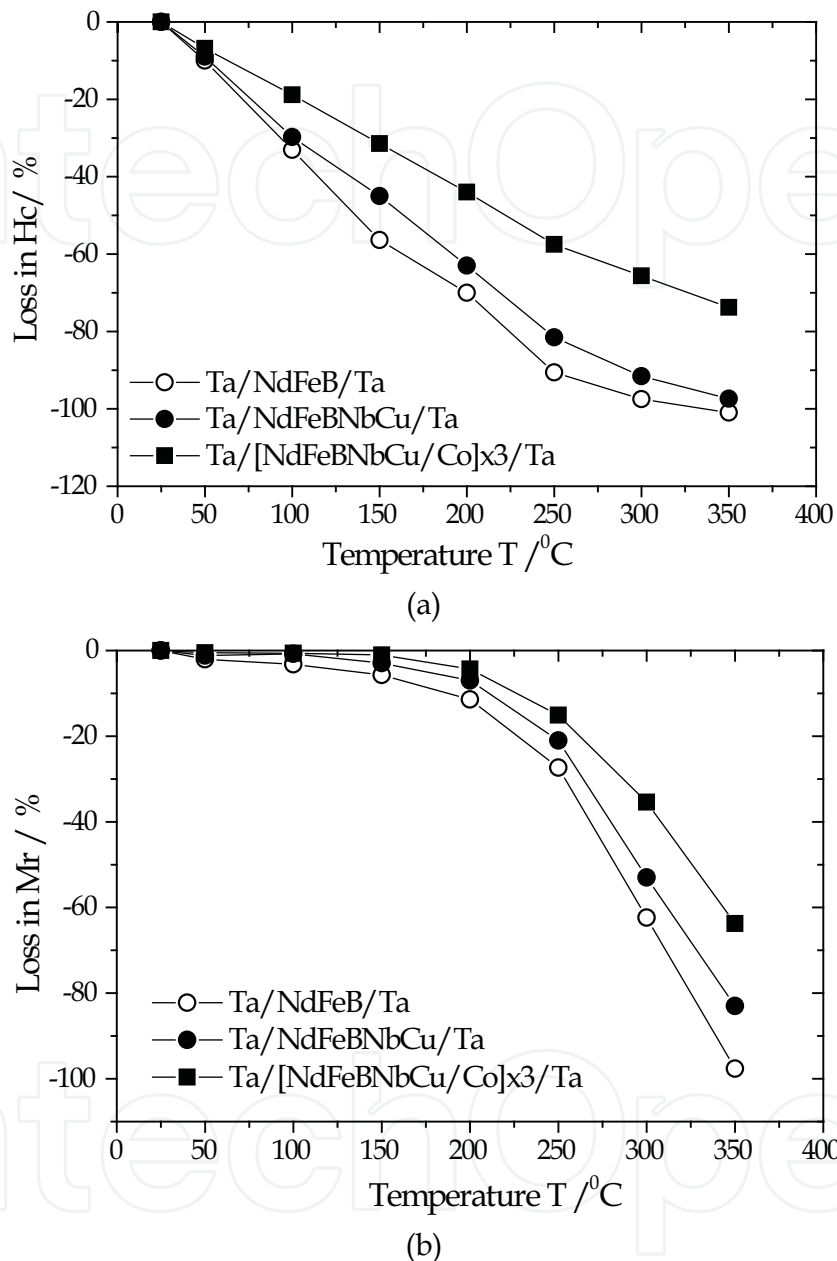


Fig. 14. The evolution of the coercivity (a) and remanence magnetization (b) as a function of temperature for Ta/NdFeB/Ta, Ta/NdFeBNbCu/ and Ta/[NdFeBNbCu/Co] $\times$ 3 films.

## 7. Conclusion

In nanocomposite magnetic materials, the ferromagnetic exchange interaction between the soft and Nd<sub>2</sub>Fe<sub>14</sub>B hard magnetic phases is largely influenced by the phase distribution, phase boundary conditions and grain size. Many attempts were made to improve the hard magnetic properties of nanocomposite permanent magnets.

In this chapter, a brief review on the influence of the additions such as, Nb and Cu, Co and Si, on the structure and hard magnetic properties of Nd-Fe-B nanocomposite thin films is presented, especially describing our recent results. Our results was mainly focused on the controlling the nanostructures by stratification of Nd-Fe-B-Nb-Cu magnetic layer and simultaneously addition of Co or Fe-Si-B as spacer layer.

For Nd-Fe-B thin films, the combined addition of Cu and Nb (Cu/Nb ratio of 1/3) in the Nd-Fe-B film and together with the use of the Co layers for stratification of the Nd-Fe-B-Nb-Cu layer are very effective tools for improving the coercivity and remanence values and for the increase of the Curie temperature. As compared to Ta/NdFeBNbCu(540nm)/Ta magnetic single layer, the multilayer Ta/[NdFeBNbCu(180nm)/Co(2nm)]x3/Ta thin film annealed at 650°C for 20 minutes exhibits very good hard magnetic properties such as coercivity of about 22.7 kOe and remanent magnetization of about 100.6 emu/g. The replacement of Fe by a small Co amount (about 1.5% from the total volume of multilayer [NdFeBNbCu(180nm)/Co(2nm)]x3 system) significantly increases the Curie temperature with about 68°C.

As a result of the stratification effect of Nd-Fe-B-Nb-Cu by using Fe-B-Si as spacer layer, the multilayer Ta/[NdFeBNbCu (180nm)/FeBSi(15nm)]x3/Ta thin film annealed at 680°C for 20 minutes exhibits very good hard magnetic properties such as: coercivity of about 22.8 kOe, saturation magnetisation of about 127.4 emu/g, remanent magnetisation of about 117.8 emu/g, an increase in Curie temperature of about 17°C, due to a strong exchange coupling between soft and hard magnetic phases. These samples present a more rectangular hysteresis loops.

We have demonstrated that, the directly inclusion in the Nd-Fe-B film volume of combined addition of Nb and Cu and stratification of Nd-Fe-B-Nb-Cu film by use of Co or Fe-Si-B film as spacer layer lead to the improvement of the hard magnetic properties of Nd-Fe-B films. A disadvantage of these samples regards the poor reproducibility of the magnetic properties since composite sputtering targets were used. Therefore, some of the future work within this topic will focus on the reproducibility of the magnetic properties by the use of the co-deposition from elemental targets.

## 8. Acknowledgements

Support from the Romanian NUCLEU Programme (Contract PN 09 43-project PN 02 01) and Ideas Programme /CNCSIS/(Contract 744/2009)/ Ministry of Education, Research, Youth and Sport is highly acknowledged.

## 9. References

- Ao Q., Zhang W.L. and Wu J.S., (2006). Exchange coupling and remanence enhancement in nanocomposite Nd-Fe-B/FeCo multilayer films, *J. Magn. Magn. Mater.* Vol. 229, Issue 2, p.440-444, ISSN: 0304-8853.
- Chang W. C., Wang S. H., Chang S. J., Tsai M. Y. and Ma B. M., (1999). The Effects of Refractory Metals on the Magnetic Properties of  $\alpha$ -Fe/R<sub>2</sub>Fe<sub>14</sub>B-type Nanocomposites, *IEEE Trans. Magn.*, Vol. 35, No.5, p. 3265-3267, ISSN: 0018-9464.
- Chang H. W., Shih M. F., Chang C. W., Hsieh C. C., Fang Y. K., and Chang W. C., Sun A. C., (2008). Magnetic properties and microstructure of directly quenched

- $\text{Nd}_{9.5}\text{Fe}_{75.5-x}\text{M}_x\text{B}_{15}$  (M = Mo, Nb, Ta, Ti, V, and Zr; x = 0-4) bulk magnets, *J. Appl. Phys.*, Vol. 103, 07E105, ISSN: 0021-8979.
- Chang H. W., Cheng Y. T., Chang C. W., Hsieh C. C., Guo Z. H., Chang W. C., and Sun A. C., (2009). Improvement of size and magnetic properties of  $\text{Nd}_{9.5}\text{Fe}_{72.5}\text{Ti}_3\text{B}_{15}$  bulk magnets by Zr or Nb substitution for Ti, *J. Appl. Phys.*, Vol. 105, 07A742, ISSN: 0021-8979.
- Chen Yun-Zhong, He Shu-li, Zhang Hong-Wei, Chen Ren-Jie, Rong Chuan-Bing, Sun Ji-Rong and Shen Bao-Gen, (2006). Magnetic properties of nanocomposite  $\text{Pr}_2(\text{FeCo})_{14}\text{B}/\alpha\text{-(FeCo)}$  with addition of Sn, *J. Phys. D: Appl. Phys.*, Vol. 39, p. 605-609, ISSN: 0022-3727.
- Chiriac H. and Marinescu M., (1998). Magnetic properties of  $\text{Nd}_8\text{Fe}_{77}\text{Co}_5\text{B}_6\text{CuNb}_3$  melt-spun ribbons, *J. Appl. Phys.*, Vol. 83, No.11, p.6629-6630, ISSN: 0021-8979.
- Chiriac H., Marinescu M., Buschow K.H.J., de Boer F.R., Bruk E., (1999). Nanocrystalline  $\text{Nd}_8\text{Fe}_{77}\text{Co}_5\text{CuNb}_3\text{B}_6$  melt-spun ribbons, *J. Magn. Magn. Mater.*, Vol. 203, p. 153-155, ISSN: 0304-8853.
- a-Chiriac H., Grigoras M. and Urse M., (2007). Influence of the spacer layer on microstructure and magnetic properties of  $[\text{NdFeB}/(\text{NbCu})] \times n$  thin films, *J. Magn. Magn. Mater.*, Vol. 316, Issue 2, p. e128-131, ISSN: 0304-8853.
- b- Chiriac H., Grigoras M., Urse M., (2007). The Co content and stratification effect on the magnetic properties, microstructure, and phase evolution of  $[\text{NdFeBNbCu}/\text{Co}] \times n$  thin films, *J. Appl. Phys.*, Vol.101, 09k523, ISSN: 0021-8979.
- Chiriac H., Grigoras M., Lupu N., Urse M., and Buta V., (2008). The Hard Magnetic Properties and Microstructure Evolution of the Multilayer  $[\text{NdFeBNbCu}/\text{FeBSi}] \times n$  Thin Films, *J. Appl. Phys.*, Vol. 103, 07E144, ISSN: 0021-8979.
- Chiriac H., H; Grigoras M., Urse M., Lupu N., (2009). Enhancement of the Thermal Stability of NdFeB Thin Films for Micro-Electro- Mechanical Systems Applications, *Sensor Letters*, Vol.7, Issue 3, p. 251-254, ISSN: 1546-198X.
- Coe J.M.D., (1996). Rare Earth Iron Permanent Magnets, J.M.D. Coey (ed.). Clarendon Press., Oxford, UK.
- Cui B.Z., Sun X.K., Liu W., Zhang Z.D., Geng D.Y., and Zhao X.G., (2000). Effects of additional elements on the structure and magnetic properties of  $\text{Nd}_2\text{Fe}_{14}\text{B}/\alpha\text{-Fe}$ -type nanocomposite magnets, *J. Phys. D: Appl. Phys.*, Vol. 33, p. 338-344, ISSN: 0022-3727.
- Cui B. Z., and O'Shea M. J., (2003). Exchange coupling and magnetic properties of  $\text{Nd}_2\text{Fe}_{14}\text{B}/\text{Co}$  nanocomposite thin films, *J. Magn. Magn. Mater.*, Vol. 256, Issues 1-3, p. 348-354, ISSN: 0304-8853.
- Cui B. Z., Huang M. Q., Yu R. H., Kramp A., Dent J., Miles D.D. and Liu S., (2003). Magnetic properties of  $(\text{Nd,Pr,Dy})_2\text{Fe}_{14}\text{B}/\alpha\text{-Fe}$  nanocomposite magnets crystallized in a magnetic field, *J. Appl. Phys.* Vol. 93, p. 8128-8130, ISSN: 0021-8979.
- Cui B.Z., and O'Shea M. J., (2004). Hard magnetic properties of rapidly annealed NdFeB/Co films and intergrain interactions, *J. Magn. Magn. Mater.*, Vol. 279, Issue 1, p. 27-35, ISSN: 0304-8853.
- Cui B. Z., Yu C. T., Han K., Liu J. P., Garmestani H., Pechan M. J., Schneider-Muntau H. J., (2005). Magnetization reversal and nanostructure refinement in magnetically

- annealed Nd<sub>2</sub>Fe<sub>14</sub>B/ $\alpha$ -Fe-type nanocomposites, *J. Appl. Phys.* Vol. 97, 10F308, ISSN: 0021-8979.
- Fukunaga H., Kuma J., Kanai Y., (1999). Effect of strength of intergrain exchange interaction on magnetic properties of nanocomposite magnets, *IEEE Trans. Magn.*, Vol. 35, Issue: 5, pp. 3235-3240, ISSN: 0018-9464.
- Fidler J., and Schrefl T., (2000). Micromagnetic modeling-the current state of the art, *J. Phys. D: Appl. Phys.*, 33 (2000) R135-R156, ISSN: 0021-8979.
- Ghidini M., Asti G., Pellicelli R., Pernechele C., Solzi M., (2007). Hard-soft composite magnets, *J. Magn. Magn. Mater.*, Vol. 316, p. 159-165, ISSN: 0304-8853.
- Hadjipanayis G. C., (1999). Nanophase hard magnets, *J. Magn. Magn. Mater.*, Vol. 200, p. 373-391, ISSN: 0304-8853.
- Harland C. L. and Davies H. A., (2000). Effect of Co and Zr on magnetic properties of nanophase PrFeB alloys, *J. Appl. Phys.* Vol. 87, p. 6116, ISSN: 0021-8979.
- Hirosawa S., Kanekiyo H., and Uehara M., (1993). High-Coercivity Iron-Rich Rare-Earth Permanent-Magnet Material Based on (Fe,Co)<sub>3</sub>B-Nd-M (M= Al, Si, Cu,Ga, Ag, Au), *J. Appl. Phys.*, Vol. 73, p. 6488-6490, ISSN: 0021-8979.
- Ishii R., Miyoshi T., Kanekiyo H., Hirosawa S., (2007). High-coercivity nanocomposite permanent magnet based on Nd-Fe-B-Ti-C with Cr addition for high-temperature applications, *J. Magn. Magn. Mater.*, Vol. 312, p. 410-413, ISSN: 0304-8853.
- Jiang H., O'Shea M.J., (2000). Structure and magnetic properties of NdFeB thin films with Cr, Mo, Nb, Ta, Ti, and V buffer layers, *J. Magn. Magn. Mater.*, Vol. 212, p. 59-68, ISSN: 0304-8853.
- Jiang J. S., Pearson J. E., Liu Z. Y., Kabius B., Trasobares S., Miller D. J., Bader S. D., Lee D. R., Haskel D., Srajer G. and Liu J. P., (2004). Improving exchange-spring nanocomposite permanent magnets, *Applied Phys. Letters*, Vol. 85, No.22, p.5295-5293, ISSN: 0003-6951.
- Jurczyk M., Jakubowicz J., (2000). Improved temperature and corrosion behaviour of nanocomposite Nd-2(Fe,Co,M)(14)B/ $\alpha$ -Fe magnets, *J. Alloy Compd.*, Vol. 311, Issue: 2, pp. 292-298, ISSN: 0925-8388.
- Jurczyk M. and Wallace W. E., (1986). Magnetic-Behavior of R<sub>1.9</sub>Zr<sub>0.1</sub>Fe<sub>14</sub>B and R<sub>1.9</sub>Zr<sub>0.1</sub>Fe<sub>12</sub>Co<sub>2</sub>B Compounds, *J. Magn. Magn. Mater.* Vol. 59, p. L182-1986, ISSN: 0304-8853.
- Kanekiyo H., Hirosawa S., (1998). Thick Fe<sub>3</sub>B/Nd<sub>2</sub>Fe<sub>14</sub>B nanocomposite permanent magnet flakes prepared by slow quenching, *J. Appl. Phys.*, Vol. 83, p. 6265-6267, ISSN: 0021-8979.
- Klug H.P., Alexander L.E., (1974). X ray Diffraction Procedures for Polycrystalline and Amorphous Materials, Wiley, New York, pp. 665.
- Kneller E. F. and Hawig R., (1991). The Exchange - Spring Magnet - A New Material Principle for Permanent - Magnets, *IEEE Trans. Magn.*, Vol. 27, p. 3588-3600, ISSN: 0018-9464.
- Lemke H., Lang T., Goddenhenrich T., (1995). Micro Patterning of the Thin Nd-Fe-B Films, *J. Magn. Magn. Mater.*, Vol. 148, p. 426-432, ISSN: 0304-8853.

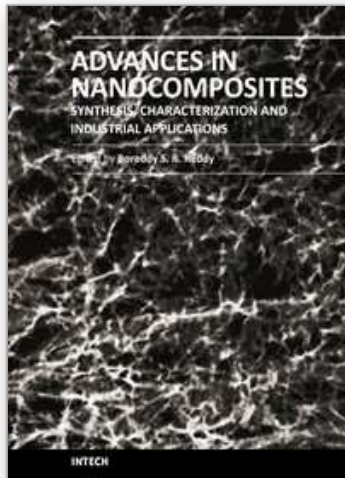
- Lileev A.S., Parilov A.A., Blatov V.G., (2002). Properties of hard magnetic Nd-Fe-B films versus different sputtering conditions, *J. Magn. Magn. Mater.*, Vol.242-245, p.1300-1303, ISSN: 0304-8853.
- Liu W., Zhang Z. D., Liu J. P., Dai Z. R., Wang Z. L., Sun X. K., and Sellmyer D. J., (2003). Nanocomposite (Nd,Dy)(Fe,Co,Nb,B)<sub>5.5/a</sub>-Fe multilayer magnets with high performance, *J. Phys. D: Appl. Phys.*, Vol. 36, p. L63-L66 PII: S0022-3727(03)60573-5, RAPID COMMUNICATION, ISSN: 0021-8979.
- Liu Z .W., and Davies H. A., (2007). Irreversible magnetic losses for melt-spun nanocrystalline Nd/Pr-(Dy)-Fe/Co-B ribbons, *J. Phys. D: Appl. Phys.*, Vol. 40, p. 315-319, ISSN: 0022-3727.
- Manaf A., Buckley R.A., Davies H.A., (1993). New nanocrystalline high-remanence Nd-Fe-B alloys by rapid solidification, *J. Magn. Magn. Mater.*, Vol.128, p.302-306 , ISSN: 0304-8853.
- Matsuura Y., Hirosawa S., Yamamoto H., Fujimura S., and Sagawa M., (1985). Magnetic properties of the Nd<sub>2</sub>(Fe<sub>1-x</sub>Co<sub>x</sub>)<sub>14</sub>B system, *Appl. Phys. Lett.* Vol. 46, p. 308-310, ISSN: 0003-6951.
- Miyoshi T., Kanekiyo H., Hirosawa S., (2000) in: H. Kaneko, M. Homma, M. Okada (Eds.), *Proceedings of Sixteenth International Workshop on Rare-Earth Magnets and their Applications*, The Japan Institute of Metals, 2000, p. 495.
- Ping D. H., Hono K., Kanekiyo H., and Hirosawa S., (1999). Microstructural Evolution of Fe<sub>3</sub>B/Nd<sub>2</sub>Fe<sub>14</sub>B Nanocomposite Magnets Microalloyed with Cu and Nb, *Acta Mater.* Vol. 47, No. 18, p. 4641-4651, ISSN: 1359-6454.
- Ping D. H., Wu Y. Q., Kanekiyo H., Hirosawa S., and Hono K., (2000). Microstructure and Hard Magnetic Properties of Cu and Nb Containing Nd-Fe-B Nanocomposites, *Proceedings of the 16th International Workshop on Rare Earth Magnets and their Applications*, September 10 - 13, 2000, Sendai, Japan.
- Rajasekhara M., Akhtara D., Manivel Rajaa M., Ramb S., (2008). Effect of Mn on the magnetic properties of Fe<sub>3</sub>B/Nd<sub>2</sub>Fe<sub>14</sub>B nanocomposites, *J. Magn. Magn. Mater.*, Vol. 320, p.1645-1650, ISSN: 0304-8853.
- Rama Rao N.V., Gopalan R., Manivel Raja M., Chandrasekaran V., Chakravarty D., Sundaresan R., Ranganathan R., Hono K., (2007). Structural and magnetic studies on spark plasma sintered SmCo<sub>5</sub>/Fe bulk nanocomposite magnets, *J. Magn. Magn. Mater.*, Vol. 312, p.252-257, ISSN: 0304-8853.
- Schrefl T., Fidler J., Editor(s): Coey M., Lewis L.H., Ma B.M., Schrefl T., Schultz L., Fidler J., Harris V.G., Hasegawa R., Inoue A., McHenry M., (1999). Micromagnetics of nanocrystalline permanent magnets, *ADVANCED HARD AND SOFT MAGNETIC MATERIALS*, *Book Series: Materials Research Society Symposium Proceedings*, Vol. 577, p. 163-174.
- Schrefl T., Fidler J., and Suess D., (2000). Micromagnetic modelling of nanocomposite magnets, *Proc. XI. Int. Symp. on Magnetic Anisotropy and Coercivity in Rare Earth Transition Metal Alloys*, Ed. H. Kaneko, M. Homma, M. Okada, The Japan Institute of Metals, Sendai, Japan, p. S57-S71.
- Shandong L., Gu B. X., Sen Y., Hong Bi, Yaodong D., Zongjun T., Guozhi X., Youwei D., and Zuanru Y., (2002). Thermal behaviour and magnetic properties of B-rich NdFeB

- nanocomposite hard magnetic alloys with partial substitution of Dy for Nd, *J. Phys. D: Appl. Phys.*, Vol. 35, p. 732-737, ISSN: 0022-3727.
- Shindo M., Ishizone M., Sakuma A., Kato H. and Miyazaki T., (1997). Magnetic properties of exchange-coupled  $\alpha$ -Fe/Nd-Fe-B multilayer thin-film magnets, *J. Appl. Phys.* Vol. 81, p. 4444-4446, ISSN: 0021-8979.
- Shull R.D., (2007). Nanocrystalline and Nanocomposite Magnetic Materials and Their Applications, *J. Iron Steel Res. Int.*, 14(4) p. 69-74, ISSN 1006-706X.
- Skomski R., Hadjipanayis G. C., and Sellmyer D. J., (2009). Graded permanent magnets, *J. Appl. Phys.*, Vol. 105, 07A733, ISSN: 0021-8979.
- Sun Y., Liu M., Han G.B., Gao R.W., (2008). Anisotropy at nano-grain boundary and effective anisotropy between magnetically soft and hard nano-grains, *J. Magn. Magn. Mater.*, Vol. 320, p. 760-762, ISSN: 0304-8853.
- Tsai J.L., Chin T.S., and Kronmüller H., (2000). *Proceedings of Sixteenth International Workshop on Rare-Earth Magnets and Their Applications*, Edited by H. Kaneko, M.Homma, M.Okada, The Japan Institute of Metals.
- Tsai J-L., Yao Y-D., Chin T-S., and Kronmüller H., (2002). Spacer layer effect and microstructure on multi-layer  $[\text{NdFeB}/\text{Nb}]_n$  films, *J. Magn. Magn. Mater.*, Vol. 239, Issues 1-3, p. 450-452, ISSN: 0304-8853.
- Van Khoa T., Ha N.D., Hong S.M., Jin H.M., Kim G.W., Hien T.D., Tai L.T., Duong N.P., Lee K.E., Kim C.G., Kim C.O., (2006). Composition dependence of crystallization temperature and magnetic property of NdFeB thin films, *J. Magn. Magn. Mater.*, Vol. 304, p. e246-e248, ISSN: 0304-8853.
- Van Khoa T., Tai L.T., Hien T.D., Duong N.P., Kim C.O., (2008). Enhancement of the Curie temperature and the remanence in NdFeB/Fe multilayer films, *J. Korean Phys. Soc.*, Vol. 52, p.1677-1680, ISSN: 0374-4884.
- Walther A., Marcoux C., Desloges B., Grechishkin R., Givord D, Dempsey N.M., (2009). Micro-patterning of NdFeB and SmCo magnet films for integration into micro-electro-mechanical-systems, *J. Magn. Magn. Mater.*, Vol. 321, Issue: 6, p. 590-594, ISSN: 0304-8853.
- Wang C., Yan M., and Li Q., (2007). Crystallization kinetics, microstructure and magnetic properties of  $\text{Nd}_2\text{Fe}_{14}\text{B}/\alpha$ -Fe magnets with Zr addition, *J. Phys. D: Appl. Phys.*, Vol. 40, p. 3551-3556, ISSN: 0022-3727.
- Wang H.-Y., Zhao F.-A., Chen N.-X., Liu G., (2005). Theoretical investigation on the phase stability of  $\text{Nd}_2\text{Fe}_{14}\text{B}$  and site preference of V, Cr, Mn, Zr and Nb, *J. Magn. Magn. Mater.*, Vol. 295, p. 219-229, ISSN: 0304-8853.
- Withanawasam L., Murphy A.S., Hadjipanayis G.C., and Krause R.F., (1994). Nanocomposite  $\text{R}_2\text{Fe}_{14}\text{B}/\text{Fe}$  Exchange-Coupled Magnets, *J. Appl. Phys.* Vol. 76, p.7065-7067, ISSN: 0021-8979.
- Xiong X. Y., Hono K., Hirosawa S. and Kanekiyo H., (2002). Effects of V and Si additions on the coercivity and microstructure of nanocomposite  $\text{Fe}_3\text{B}/\text{Nd}_2\text{Fe}_{14}\text{B}$  magnets, *J. Appl. Phys.*, Vol. 91, No.11, p. 9308-9314, ISSN: 0021-8979.
- Zhang P. Y., Hiergeist R., Albrecht M., Braun K.-F., Sievers S., Lüdke J., and Ge H. L., (2009). Enhancement in the coercivity in  $\text{Nd}_2\text{Fe}_{14}\text{B}/\alpha$ -Fe nanocomposite alloys by Ti doping, *J. Appl. Phys.* Vol. 106, p. 073904, ISSN: 0021-8979.

Yang C. J. and Kim S.W., (1999). Observations of exchange coupling in Nd<sub>2</sub>Fe<sub>14</sub>B/Fe/Nd<sub>2</sub>Fe<sub>14</sub>B sandwich structures and their magnetic properties, *J. Magn. Magn. Mater.*, Vol. 202, p. 311-320, ISSN: 0304-8853.

IntechOpen

IntechOpen



## **Advances in Nanocomposites - Synthesis, Characterization and Industrial Applications**

Edited by Dr. Boreddy Reddy

ISBN 978-953-307-165-7

Hard cover, 966 pages

**Publisher** InTech

**Published online** 19, April, 2011

**Published in print edition** April, 2011

Advances in Nanocomposites - Synthesis, Characterization and Industrial Applications was conceived as a comprehensive reference volume on various aspects of functional nanocomposites for engineering technologies. The term functional nanocomposites signifies a wide area of polymer/material science and engineering, involving the design, synthesis and study of nanocomposites of increasing structural sophistication and complexity useful for a wide range of chemical, physicochemical and biological/biomedical processes. "Emerging technologies" are also broadly understood to include new technological developments, beginning at the forefront of conventional industrial practices and extending into anticipated and speculative industries of the future. The scope of the present book on nanocomposites and applications extends far beyond emerging technologies. This book presents 40 chapters organized in four parts systematically providing a wealth of new ideas in design, synthesis and study of sophisticated nanocomposite structures.

### **How to reference**

In order to correctly reference this scholarly work, feel free to copy and paste the following:

Urse Maria, Grigoras Marian, Lupu Nicoleta and Chiriac Horia (2011). Nd-Fe-B Nanocomposite Thin Films: Influence of the Additions on the Structure and Hard Magnetic Properties, *Advances in Nanocomposites - Synthesis, Characterization and Industrial Applications*, Dr. Boreddy Reddy (Ed.), ISBN: 978-953-307-165-7, InTech, Available from: <http://www.intechopen.com/books/advances-in-nanocomposites-synthesis-characterization-and-industrial-applications/nd-fe-b-nanocomposite-thin-films-influence-of-the-additions-on-the-structure-and-hard-magnetic-prope>

**INTECH**  
open science | open minds

### **InTech Europe**

University Campus STeP Ri  
Slavka Krautzeka 83/A  
51000 Rijeka, Croatia  
Phone: +385 (51) 770 447  
Fax: +385 (51) 686 166  
[www.intechopen.com](http://www.intechopen.com)

### **InTech China**

Unit 405, Office Block, Hotel Equatorial Shanghai  
No.65, Yan An Road (West), Shanghai, 200040, China  
中国上海市延安西路65号上海国际贵都大饭店办公楼405单元  
Phone: +86-21-62489820  
Fax: +86-21-62489821

© 2011 The Author(s). Licensee IntechOpen. This chapter is distributed under the terms of the [Creative Commons Attribution-NonCommercial-ShareAlike-3.0 License](#), which permits use, distribution and reproduction for non-commercial purposes, provided the original is properly cited and derivative works building on this content are distributed under the same license.

IntechOpen

IntechOpen